

Carbon mass-balance modelling and carbon isotope exchange processes in dynamic caves

Silvia Frisia^{a,*}, Ian J. Fairchild^b, Jens Fohlmeister^c, Renza Miorandi^d,
Christoph Spötl^e, Andrea Borsato^{a,d}

^a School of Environmental and Life Sciences, University of Newcastle, Callaghan 2308 NSW, Australia

^b School of Geography, Earth and Environmental Sciences, University of Birmingham, Edgbaston, Birmingham B15 2TT, UK

^c Heidelberger Akademie der Wissenschaften, Im Neuenheimer Feld 229, 69120 Heidelberg, Germany

^d Museo Tridentino di Scienze Naturali, Via Calepina 14, 38100 Trento, Italy

^e Institut für Geologie und Paläontologie, Leopold-Franzens-Universität, Innsrain 52, 6020 Innsbruck, Austria

Received 5 May 2010; accepted in revised form 19 October 2010; available online 2 November 2010

Abstract

Diverse interpretations have been made of carbon isotope time series in speleothems, reflecting multiple potential controls. Here we study the dynamics of ^{13}C and ^{12}C cycling in a particularly well-constrained site to improve our understanding of processes affecting speleothem $\delta^{13}\text{C}$ values. The small, tubular Grotta di Ernesto cave (NE Italy) hosts annually-laminated speleothem archives of climatic and environmental changes. Temperature, air pressure, pCO_2 , dissolved inorganic carbon (DIC) and their C isotopic compositions were monitored for up to five years in soil water and gas, cave dripwater and cave air. Mass-balance models were constructed for CO_2 concentrations and tested against the carbon isotope data. Air advection forces winter pCO_2 to drop in the cave air to ca. 500 ppm from a summer peak of ca. 1500 ppm, with a rate of air exchange between cave and free atmosphere of approximately 0.4 days. The process of cave ventilation forces degassing of CO_2 from the dripwater, prior to any calcite precipitation onto the stalagmites. This phase of degassing causes kinetic isotope fractionation, i.e. ^{13}C -enrichment of dripwater whose $\delta^{13}\text{C}_{\text{DIC}}$ values are already higher (by about 1‰) than those of soil water due to dissolution of the carbonate rock. A subsequent systematic shift to even higher $\delta^{13}\text{C}$ values, from -11.5‰ in the cave drips to about -8‰ calculated for the solution film on top of stalagmites, is related to degassing on the stalagmite top and equilibration with the cave air. Mass-balance modelling of C fluxes reveals that a very small percentage of isotopically depleted cave air CO_2 evolves from the first phase of dripwater degassing, and shifts the winter cave air composition toward slightly more depleted values than those calculated for equilibrium. The systematic ^{13}C -enrichment from the soil to the stalagmites at Grotta di Ernesto is independent of drip rate, and forced by the difference in pCO_2 between cave water and cave air. This implies that speleothem $\delta^{13}\text{C}$ values may not be simply interpreted either in terms of hydrology or soil processes.

© 2010 Elsevier Ltd. All rights reserved.

1. INTRODUCTION

The carbon stable isotope ($\delta^{13}\text{C}$) in marine carbonates is applied widely, being used to tackle issues such as the level of past atmospheric CO_2 and the character of ocean circulation (e.g. Shackleton et al., 1983; Berner, 2006). In continental carbonates, the significance of the $\delta^{13}\text{C}$ values may

serve as an indicator of the bioproductivity and/or hydrology of lakes (Leng and Marshall, 2004), atmospheric pCO_2 based on calcretes formed in arid regions (Cerling, 1984), or recharge by using riverine tufas (Andrews, 2006). An understanding of the local context, however, is commonly required. In cave secondary mineral deposits known as speleothems, $\delta^{13}\text{C}$ is less widely utilized than $\delta^{18}\text{O}$ as a proxy of environmental and climate changes (McDermott, 2004; McDermott et al., 2005; Lachniet, 2009). Carbon isotope ratios of speleothem calcite, however, have potential for

* Corresponding author. Tel.: +61 2 4921 5402.

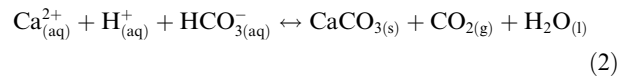
E-mail address: silvia.frisia@newcastle.edu.au (S. Frisia).

the reconstruction of the atmospheric $p\text{CO}_2$ evolution (Baskaran and Krishnamurthy, 1993) and are a proxy of palaeovegetation (Dorale et al., 1992) and climate-related soil CO_2 production (Salomons and Mook, 1986; Bar-Matthews et al., 1997). The tremendous importance of $\delta^{13}\text{C}$ variability through time in speleothem-based climate reconstructions became fully apparent when Genty et al. (2003) precisely identified timing, duration, and consequences of Dansgaard–Oeschger (DO) events within the last glacial cycle using $\delta^{13}\text{C}$ in a single stalagmite from SW France. In this carbon isotope record, DO events were more clearly expressed than in the $\delta^{18}\text{O}$ profile, with low $\delta^{13}\text{C}$ values coinciding with high (warm) $\delta^{18}\text{O}$ values recorded by Greenland ice cores. The low $\delta^{13}\text{C}$ values of speleothem calcite were related to a higher proportion of isotopically light soil CO_2 dissolved in the infiltration waters during warm periods. Subsequently, Genty et al. (2006) used the carbon isotopic composition of three mid-latitude stalagmites from France and Tunisia to reconstruct climate-related changes in soil and vegetation activity during the last deglaciation. Changes in $\delta^{13}\text{C}$ values were synchronous in the three speleothems and coincided with climate events recorded in the $\delta^{18}\text{O}$ time series from Greenland ice cores. The relevance of $\delta^{13}\text{C}$ as a global palaeoclimate proxy, however, could not be unequivocally established, because kinetic fractionation likely occurred during CO_2 degassing (Genty et al., 2003). The effect of kinetic fractionation on $\delta^{13}\text{C}$ values of speleothem calcite has commonly been considered to be relatively small and it was implicitly accepted that degassing can be described in terms of equilibrium isotopic fractionation (Hendy, 1971; Salomons and Mook, 1986). This assumption was challenged by Dulinski and Rozanski (1990) who stated that the initial phase of degassing from a solution in a cave, without calcite precipitation, involves the fast release from the solution of isotopically light carbon dioxide without back-reaction occurring. The model proposed by Dulinski and Rozanski (1990) implies that in this initial phase of degassing, strong kinetic fractionation should result in an increase of $\delta^{13}\text{C}_{\text{DIC}}$ values. This first phase is followed by a slower release of isotopically light C and a slower increase of $\delta^{13}\text{C}_{\text{DIC}}$ of the solution in response to combined calcite precipitation and continued CO_2 -outgassing which, as in the first phase, was treated as a kinetic process with CO_2 only moving from liquid to gas (Dulinski and Rozanski, 1990). It has remained unclear, however, whether the carbon isotope increases associated with this one-way reaction inferred from the model actually occur in nature.

Degassing depends on the difference between the partial pressure of $p\text{CO}_2$ in the cave water and the air. Commonly, CO_2 is lost from seepage water bodies, drops or films to the gaseous phase (cave air) because the seepage water entering the cave carries in solution biogenic CO_2 evolved in the soil zone where the concentration is up to two orders of magnitude higher than in the free atmosphere (Dulinski and Rozanski, 1990; Kaufmann, 2003), according to the reactions:



The reaction combine to release isotopically light carbon dioxide to the cave air, and the release is faster the higher the difference between the $p\text{CO}_2$ in the water and in the cave air (Dulinski and Rozanski, 1990). The solution on the speleothem surface therefore becomes progressively enriched in ^{13}C with respect to the initial solution, and calcite forming from this water according to the reaction



is expected to be isotopically heavier than DIC of the infiltration water. This in-cave ^{13}C -enrichment can thus severely modify, or possibly even conceal an underlying climatically forced C isotope signal (Genty et al., 2006).

Modelling of $\delta^{13}\text{C}$ values of speleothem calcite grown in isotopic disequilibrium has, so far, focussed on the evolution of carbon isotope values in the bicarbonate of the solution wetting stalagmites in the attempt to quantify the climate-related parameter responsible for disequilibrium. The evolution of the C isotopic composition in the solution layer during degassing was calculated by Mühlinghaus et al. (2007) using a kinetic Rayleigh fractionation process (Salomons and Mook, 1986). In their model, the dominant parameter was the temporal evolution of bicarbonate on the stalagmite surface, whereas possible changes in the bicarbonate due to degassing at the stalactite tip were not considered. The drip interval, therefore, becomes the key parameter in their model influencing isotopic enrichment in ^{13}C in the solution layer at the top of a stalagmite. Mühlinghaus et al. (2008) subsequently modelled past drip-rate variability by applying an inverse model to stalagmite $\delta^{13}\text{C}$ time-series. Critically, the drip intervals used in their model are theoretical, very high (in the order of 1000 s) and not commonly measured in natural cave environments. In particular, the extreme end-members used in their model (1000–2000 s) in certain cases may be too low to allow for calcite precipitation onto a stalagmite, because slow degassing related to low drip rate could result in calcite precipitation occurring preferentially at the tip of a stalactite. The processes occurring at (as well as within) stalactites, which include degassing at their tips upon emergence of the drop, have, however, received little recognition in the modelling.

The marked increase of dripwater $\delta^{13}\text{C}_{\text{dic}}$ and the concomitant decrease of $\delta^{13}\text{C}_{\text{CO}_2}$ in the cave air due to degassing forced by ventilation at Obir cave in Austria (Spötl et al., 2005) highlighted the importance of both cave air $p\text{CO}_2$ and degassing at the stalactite tip in driving C isotope exchange. Scholz et al. (2009) found a clear dependency of the final isotope ratio of the bicarbonate of the water film on the $\delta^{13}\text{C}$ of the cave atmosphere. They assumed two end-member scenarios: the unventilated and the ventilated caves. In the non-ventilated cave, the gaseous CO_2 phase is derived solely from degassing and isotopic exchange with cave CO_2 results in lower $\delta^{13}\text{C}$ values in the bicarbonate than expected from Rayleigh distillation. By contrast, in a highly ventilated cave, air $\delta^{13}\text{C}$ reaches atmospheric values (considering a mean value of -8‰ , Mook, 2006), and bicarbonate $\delta^{13}\text{C}$ is higher (i.e. $\delta^{13}\text{C} = 1.7\text{‰}$) than calculated for pure Rayleigh distillation. The approach of Scholz

et al. (2009) highlights the importance of cave air $\delta^{13}\text{C}$ in modifying the $\delta^{13}\text{C}$ of the calcite-precipitating solution layer. This opens the possibility to use the $\delta^{13}\text{C}$ of cave calcite, in favourable conditions, as a proxy of cave air pCO_2 and C isotope composition (Baskaran and Krishnamurthy, 1993). A thorough understanding of the evolution of $\delta^{13}\text{C}$ in karst systems thus becomes critically important to develop and validate inverse models which allow the reconstruction of past climate-related parameters or atmospheric changes from $\delta^{13}\text{C}$ data of stalagmites.

The evolution of C in karst systems starts at the Earth's surface, and most notably in the upper part of the soil zone, where most CO_2 dissolves in the infiltration waters (Baskaran and Krishnamurthy, 1993; Spötl et al., 2005), proceeds by host-rock dissolution and degassing at stalactite tips, or en-route to the stalactite (Spötl et al., 2005; Fairchild et al., 2007), and then by degassing (both fast and slow) and equilibration on the speleothem (stalagmite or flowstone) surface (Hendy, 1971; Dulinski and Rozanski, 1990; Dreybrodt, 2008; Romanov et al., 2008; Mühlinghaus et al., 2009; Scholz et al., 2009). In most cases, however, it is impossible to monitor the entire $\delta^{13}\text{C}$ evolution from soil water to dripwater to speleothem calcite. Mass-balance models based on analyses of cave air and water compositions including C isotopes (both stable and radiogenic) allow reconstructing C-isotope exchanges from the initial water to the stalagmite.

Here, we present a quantification of the C fluxes for Grotta di Ernesto in NE Italy using a combination of multi-annual, multi-parameter monitoring and C isotope-based mass-balance models. This cave, due to its relatively small size, good accessibility, undisturbed catchment, low tourist impact, and sealed entrance is a natural laboratory to mod-

el and quantify the contribution of the various processes on the final $\delta^{13}\text{C}$ value of the stalagmite. Our results and conclusions have implications for other cave systems and for the interpretation of $\delta^{13}\text{C}$ time series in ventilated caves.

2. STUDY SITE AND RATIONALE FOR C-FLUXES MODELLING

Grotta di Ernesto is located in northeast Italy (longitude $11^\circ39'25''$, latitude $45^\circ58'38''$) at an elevation of 1167 m above sea level (a.s.l.) on a steep, north-facing slope (Fig. 1) of the Asiago–Lavarone karst plateau, which reaches a maximum elevation of about 2300 m. Surface-air temperatures range from about -10°C to about 20°C . The mean annual rainfall since 1950 is about 1250 mm/year as recorded by the weather stations of Lavarone and Vezzena, which are located on the northern margin of the plateau, within 20 km from the cave, at about 1200 m a.s.l. The synoptic scale circulation system is the same for the northern margin of the Asiago–Lavarone–Vezzena plateau. Orographically forced mesoscale phenomena which may modify significantly synoptic features are unlikely because there are no mountain barriers between the cave site and the weather stations. With the exception of the contribution of local summer thunderstorms, the mean precipitation and temperature measured at the weather stations reflect those at the cave site (<http://meteo.iasma.it/meteo/>).

Climate in the area can be classified as mesothermic–humid with respect to the hydrological cycle (Thornton and Mather, 1955) and is of the continental–alpine type with respect to temperature (Eccel and Saibanti, 2008). The mean annual air temperature at the cave site is

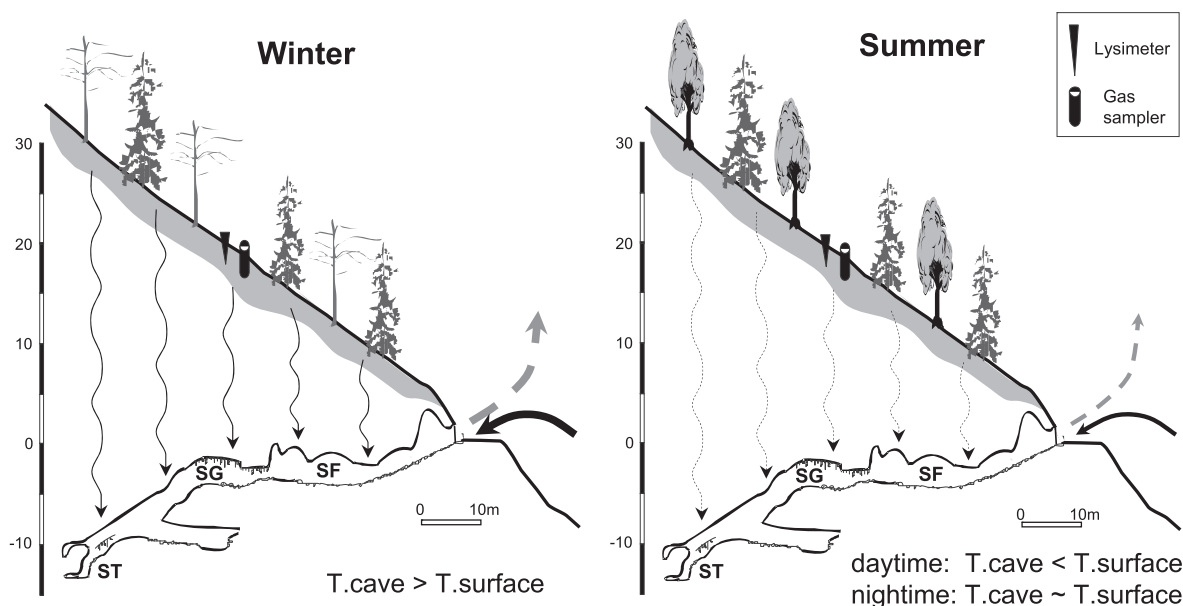


Fig. 1. N–S cross-sections showing the geometry of Grotta di Ernesto gallery, the position of the gas sampler and lysimeter at -1.5 m, and a schematic representation of cave circulation in winter and summer modes. Black, bold arrow indicates flux of external air. Dashed, bold arrow indicates flux of cave air. Thin arrows indicate flow of infiltration waters, which is more enhanced in the cool season. Key: c = cave; s = surface; SF = Sala del Focolare; SG = Sala Grande; ST = Sala Terminale.

6.7 °C, which is the same as the temperature inside the cave, which is remarkably constant throughout the year (Frisia et al., 2003). At present-day conditions, snow cover persists from early December to early March, and exceptionally until April.

The location of the cave on the northern, cool side of the valley and its position under a forest canopy result in high soil moisture and a high sensitivity of soil CO₂ production to temperature (Egli et al., 2009). These are desirable qualities to study the evolution of δ¹³C in the soil–host rock–cave–speleothem system, because soil pCO₂ production is primarily a function of temperature, and the low temperature and high humidity at this cave site limit the precipitation of calcite from infiltration waters prior to dripping onto the stalagmite (Fairchild et al., 2000). The soil above the cave has a typical thickness of about 1 m and has developed since the Early Holocene (Egli et al., 2009). It is a Rendzic Leptosol with coarse to medium texture and a gravel-rich (skeletal) C horizon, which results in relatively rapid drainage. The present-day vegetation consists of C3 plants, mostly conifers (Fairchild et al., 2009), whose finest rootlets locally penetrate the shallowest part of the cave, near the entrance.

The natural entrance to the cave, which had been concealed under a landslide, was re-opened in 1983, and access is through a locked, solid metal door. The whole cave is cut in dolomitic limestone characterized by pervasive intercrystalline porosity and fracture permeability (Miorandi et al., 2010). A descending passage (Fig. 1) connects the entrance room, located at about –5 m with respect to the surface, to a horizontal gallery at –20 m, decorated by both active and fossil speleothems. A steep descent then connects this gallery to the final room, called Sala Terminale (ST), located at –30 m.

The cave has several features which make it a perfect location for a monitoring study of C-fluxes and their influence on C-isotope exchange: (i) it is a small cave which can be easily accessed in all its parts; (ii) it does not host any cave streams which may control CO₂ degassing (Troester and White, 1984; Ek and Gewalt, 1985); (iii) it has been monitored since 1997 (Borsato, 1997; McDermott et al., 1999; Miorandi et al., 2006) and (iv) access to the site is limited and controlled. Most notably, monitoring of cave parameters was targeted to relate presence, crystal morphology and trace-element composition of annual laminae to climate, hydrology and ecosystem processes (Huang et al., 2001; Huang and Fairchild, 2001; Frisia et al., 2000, 2003, 2005; Fairchild et al., 2000, 2001, 2009; Miorandi et al., 2006, 2010; Wynn et al., 2010). This monitoring revealed a relationship between lamina thickness, seasonal pCO₂ variability in the cave atmosphere, and winter surface temperature (Frisia et al., 2000, 2003), which allowed the use of Grotta di Ernesto stalagmite lamina-thickness data to build the first speleothem-based reconstruction of Northern Hemisphere temperature variability for the past 500 years (Smith et al., 2006). This result was important enough to warrant the effort of further monitoring, and eventually to model the processes controlling C fluxes and isotope exchange throughout the soil-cave system building on the approach of Spötl et al. (2005).

3. MONITORING AND ANALYTICAL TECHNIQUES

The monitoring and sampling protocol was designed to trace the evolution of both pCO₂ and δ¹³C in air and water from the surface layers of the soil zone, to the lower soil and upper part of the upper epikarst where interaction with carbonate rock fragments occur, and finally into the cave. Measurements of soil pCO₂ commenced in October 2003, when three gas samplers were installed at depths of 0.5, 1.0 and 1.5 m in the soil just above Sala Grande (SG, Fig. 1). The first two gas samplers (0.5 and 1.0 m) were inserted in the A and B horizons, which have a loamy structure with common angular rock fragments. The 1.5 m sampler reached the deeper soil horizons where rock fragments become progressively more abundant (>20%) and the regolith. Soil pCO₂ was logged monthly by using a Draeger Multiwarn infra-red sensor instrument (accuracy ±10%, resolution 0.01%). All readings were corrected to standard atmospheric pressure (1013 hPa) according to the relationship proposed by Spötl et al. (2005): CO₂ (ppm volume) = CO₂ (measured) × 1013/pressure (measured).

Soil air samples for carbon isotope analysis were collected monthly according to the minimal-disturbance method detailed in Spötl (2004) whereby a 1 m hollow metal probe is pushed into the soil and gas is removed by slow pumping. Soil water was collected in two lysimeters located about 2 m downslope with respect to the gas samplers. Temperature was logged in the lysimeter at a depth of about 1 m to obtain a record of soil-temperature variations, which could be then compared to seasonal soil-gas and water pCO₂ data. Aliquots of soil water (when available), as well as of dripwater were sampled during each visit for δ¹³C analyses of DIC. Following the protocol of Spötl (2005), three drops of phosphoric acid were injected into a 10 mL Helium-flushed Labco exetainer followed by an aliquot of soil or dripwater (whose volume depended on the alkalinity, commonly 0.3 ml). Water (and gas) samples were immediately stored in a portable cooler and sent to Innsbruck in a gas-tight box. Mass spectrometric analyses were carried out within 48 hours of arrival of the samples.

Cave atmosphere pCO₂ concentration was measured on a monthly basis since 2004 using a Vaisala Meter GM70 with a GMP222 probe (accuracy at 25 °C ± 20 ppm CO₂). The pCO₂ was analysed at nine points along the gallery during each cave visit and also by continuous logging for a short period. These tests of continuous logging were carried out in autumn 2005, winter 2006, and autumn-winter 2007 in order to check for short-term pCO₂ variability, and in particular for the effects of visitors on the cave atmosphere. The continuous data (15-min intervals) were corrected for the barometric pressure measured continuously (10 min interval) at Passo Vezena meteorological station. In addition, each monthly visit, the atmospheric pressure was measured at the cave site with a barometer. This allowed calculating the pressure variability at the cave site during the period of continuous pCO₂ logging from the data recorded at Passo Vezena.

Before August 2007 cave air temperature was measured manually during each monthly visit. From August 2007 to

November 2008 it was logged hourly using Infraclog DK-500 data loggers (resolution 0.003 °C, precision ± 0.1 °C) placed near the entrance and in the deepest part of the cave. Cave air samples for carbon isotope analyses were collected along the whole length of the cave using Helium-flushed exetainers, following initial measurement of pCO₂. Although care was taken to avoid breath-contamination, disparity of $\delta^{13}\text{C}$ values during some sampling sessions in 2007 and 2008, despite consistent pCO₂ values, indicate that this may have occurred.

All $\delta^{13}\text{C}$ analyses were carried out at the University of Innsbruck using an on-line, continuous-flow system (Gasbench II) linked to a ThermoFisher DELTA^{plus}XL isotope ratio mass spectrometer and are reported on the VPDB scale. Calibration of the mass spectrometer was accomplished using an in-house calcite reference material whose stable isotopic composition had previously been calibrated against NBS 19, CO1, CO8, and L-SVEC (Spötl, 2004; Spötl et al., 2005). The 1 σ analytical uncertainties for $\delta^{13}\text{C}_{\text{DIC}}$ and $\delta^{13}\text{C}_{\text{air}}$ are 0.10 and 0.15 ‰, respectively.

4. RESULTS

4.1. The soil zone

Mean pCO₂ values in the soil gas above Grotta di Ernesto vary little with depth and are much higher than in the cave itself (Table 1). Carbon dioxide concentration variability in the soil gas is clearly related to seasonal surface temperatures, and the correlation between soil pCO₂ and soil temperatures is high ($R^2 = 0.86$, Fig. 2). Maximum soil pCO₂ values were measured in the warm season, from June to October (up to 12,000 ppm) and minimum values in the cold season, from November to May (300–1400 ppm at 0.5 m depth and 1500–4600 ppm at 0.5 and 1.5 m depth, respectively – see Fig. 2). A sharp drop in biogenic soil CO₂ production was observed between October and November (from about 9500 ppm to about 2000 ppm), which coincides with a decrease in soil temperature of about 2 °C. Soil monitoring data clearly indicate that in winter, when the surface temperature drops below 0 °C and the topsoil may be frozen, the temperature in the soil at depths ≥ 0.5 m is >0 °C (Fig. 2), which still allows for biogenic CO₂ production, but at reduced rates than at higher temperatures (Urbanc et al., 1997). Seasonal variability of CO₂ concentration in soil gas is more pronounced at 0.5 m than at 1.5 m depth and roughly follows the surface temperature trend (Fig. 3a) as expected from the temperature-sensitivity of bacterial decomposition of a relatively homogeneous soil organic matter (SOM) pool below

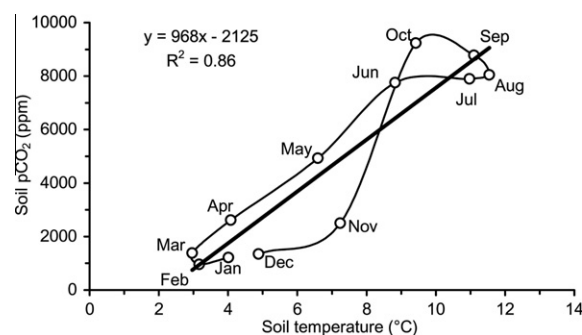


Fig. 2. Relationships between temperature measured in the soil (monthly averages) and the concentration of CO₂ in soil gas (pCO₂) above Grotta di Ernesto. A sharp decline in soil temperature from October to November is accompanied by a drop in soil CO₂ production.

25 °C (Leifeld and Fuhrer, 2005). The peak in soil CO₂ concentration commonly occurs between September and October and shows a delay of about one month (up to two months) with respect to the peak in surface temperature, at least in the gas samplers at 1.0 and 1.5 m depth (Fig. 3b).

Soil air $\delta^{13}\text{C}$ measured in the three gas sampler also show seasonal variability, with winter values of about -20 ‰ at -0.5 m and about -22 ‰ at -1.5 m and more negative values in summer, about -24 ‰ at 0.5 m depth and -25 ‰ at 1.5 m depth (Fig. 3d). The samplers at 1.0 and 1.5 m depth show muted variations with respect to the shallower sampler. When soil pCO₂ is high, the $\delta^{13}\text{C}$ of the soil air CO₂ is more negative, with the lowest values of the $\delta^{13}\text{C}$ of about -25 ‰ recorded at 1.5 m depth when soil pCO₂ was about 11,000 ppm (Fig. 4). This negative relationship between pCO₂ and air $\delta^{13}\text{C}$ characterizes most soil types in the alpine region (Urbanc et al., 1997), and is ultimately related to soil temperature. The lowest $\delta^{13}\text{C}$ values measured in the air parcels extracted from the deeper soil sampler, however, indicate that there is diffusion from the shallower soil horizons towards the surface, especially in the warm months. The deeper horizons, which include bedrock fragments and the weathered rocks, by contrast, preserve almost all the soil CO₂ produced during the warm season.

Soil water $\delta^{13}\text{C}_{\text{DIC}}$ values vary from about -12.5 ‰ in the cold season to about -17 ‰ in the warm season. These values are within the range expected for soil water HCO₃⁻ that underwent exchange with soil gas CO₂ and, being acidic, already dissolved some carbonate rock fragments in the soil with $\delta^{13}\text{C}$ values of about 1 ± 1.5 ‰ (Mook, 2006), which is the typical value of the Jurassic marine

Table 1

Mean and background level (calculated as the mean CO₂ concentration from January to March) CO_{2(gas)} concentrations of soil gas sampled at different depths, and in cave air samples for the monitoring period 2003–2007.

	Soil air pCO ₂			Cave air pCO ₂
	0.5 m	1.0 m	1.5 m	
Mean (ppm)	4722 ± 3532	4676 ± 3148	4506 ± 2411	871 ± 400
Background (January–March)	1184 ± 429	2013 ± 687	2908 ± 859	470 ± 49

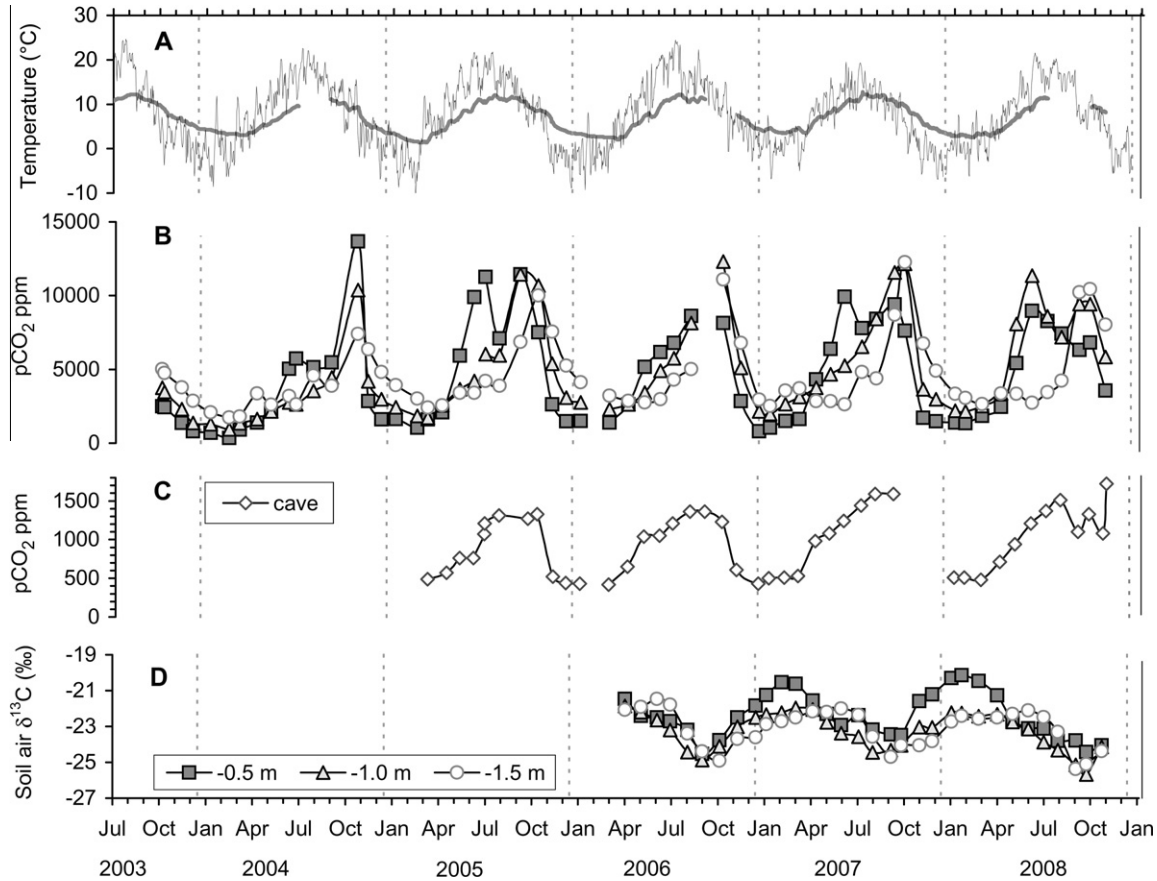


Fig. 3. Comparison between seasonal variations of surface temperature (A), soil pCO₂ measured in the three gas sampler at 0.5, 1 and 1.5 m depth in the soil above the cave (B), cave air pCO₂ since March 2005 (C) and soil air CO₂ δ¹³C (D). In A, the bold line is the monthly mean surface temperature. Some missing data in cave air measurements (C) pertain to winter months when the cave could not be accessed.

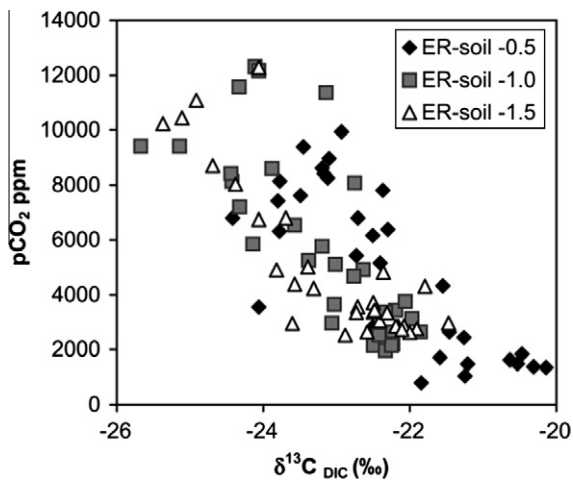


Fig. 4. Relationship between soil air pCO₂ and δ¹³C values in air samples collected within the soil samplers at 0.5, 1.0, and 1.5 m soil depth. The most negative δ¹³C values, which have been recorded in the deeper samplers (about -25‰), pertain to soil CO₂ evolved at the end of the warm season, in September and October, before the drop in temperature and soil pCO₂.

carbonate rocks in the region (Frisia and Wenk, 1993; Avanzini et al., 1997). The seasonal variability has a similar

trend as the soil air δ¹³C (Fig. 3d) with an enrichment of about +8‰. Similar δ¹³C_{DIC} values and trends recorded in alpine karst spring waters are correlated to the soil temperature in the recharge area (Urbanc et al., 1997), which influences soil CO₂ production as well as the type of vegetation. A mean value of δ¹³C_{DIC} of about -14.5‰ is typical of samples taken from the deeper lysimeter (-1.5 m), which is in contact with the skeletal horizon. This value is considered as representative of the soil waters, prior to entry into the aquifer feeding the cave drip sites and before being modified by rock-water interactions. In summary, soil monitoring data indicate that the surface temperature signal is transmitted through the soil pCO₂ variability and seasonal soil gas δ¹³C changes to the soil water δ¹³C_{DIC}.

4.2. The cave environment

On 24 of 29 sampling occasions the standard deviation of measurements taken at the nine sample sites from near the entrance to the deepest niche were within 2.5%, i.e. matched the instrumental sampling uncertainty. On only three occasions, values were slightly lower at the entrance, and on just two occasions (late September and early November 2008) there was a gradual gradient of around 300 ppm (around 800–1100 ppm) from the outer to the

innermost sampling site. The normal condition is therefore one of uniform CO_2 concentrations. The $\delta^{13}\text{C}$ values of each air sample, and the seasonal trends recorded from the entrance to the deepest chamber also show similarities (Fig. 5). In the deepest terminal chamber (ST) the $\delta^{13}\text{C}(\text{CO}_2)_{\text{gas}}$ values range from about -21‰ from April to October, when pCO_2 in the cave air is at its highest values (up to 1500 ppm CO_2 , Fig. 3c), to -13‰ from November to April, when the pCO_2 in the cave air is close to atmospheric values. The $\delta^{13}\text{C}(\text{CO}_2)_{\text{gas}}$ thus shows a trend towards higher values when the pCO_2 in the cave is low.

The pCO_2 and cave air $\delta^{13}\text{C}$ data indicating that there is no pCO_2 zonation within Grotta di Ernesto contrast with the large Belgian caves studied by Ek and Gewelt (1985), or in the shallow Ballynamintra cave (Ireland) monitored by Baldini et al. (2006), in spite of a vertical range of about 20 m. In order for this condition to apply, it follows that the CO_2 input is not localized within only one part of the cave and/or the CO_2 dispersion is very effective. An exception was found at the end of the monitoring in November 2008, when there was a steep spatial gradient from site ST at the bottom of the cave compared with the overlying Sala Grande a few days following our artificial release of carbon dioxide into the cave (see below).

Cave air pCO_2 displays seasonal variability, but with a lower amplitude than the soil pCO_2 as shown in Fig. 6. The cave pCO_2 trend is very similar to that recorded at 0.5 m depth in the soil ($r^2 = 0.95$), with a fast increase between April and June and an abrupt decrease between October and November. By contrast, pCO_2 in the deeper samplers (1.0 and 1.5 m depth) shows a more gradual increase between spring and August, and subsequently climbs to maximum values in October. This different behaviour suggests that deeper sites in the soil respond with inertia of about two months to soil heating and, consequently, to CO_2 production, whereas the cave air responds almost instantaneously to rises in surface temperature.

Tourist visits alter the pCO_2 concentration of the cave atmosphere. Summer visits are the equivalent CO_2 release of up to 100 adult person-hours per day and result in short-lived anthropogenic spikes in cave pCO_2 (Fig. 7), which can be used to model carbon dioxide fluxes. Tourist respiration results in the abrupt rise of pCO_2 from a baseline of 1300 ppm to over 1800 ppm following the visits. The higher the number of people, the higher the CO_2 concentration increases in the cave air. The subsequent return to the baseline of cave air pCO_2 values typical of the warm season occurs within two days.

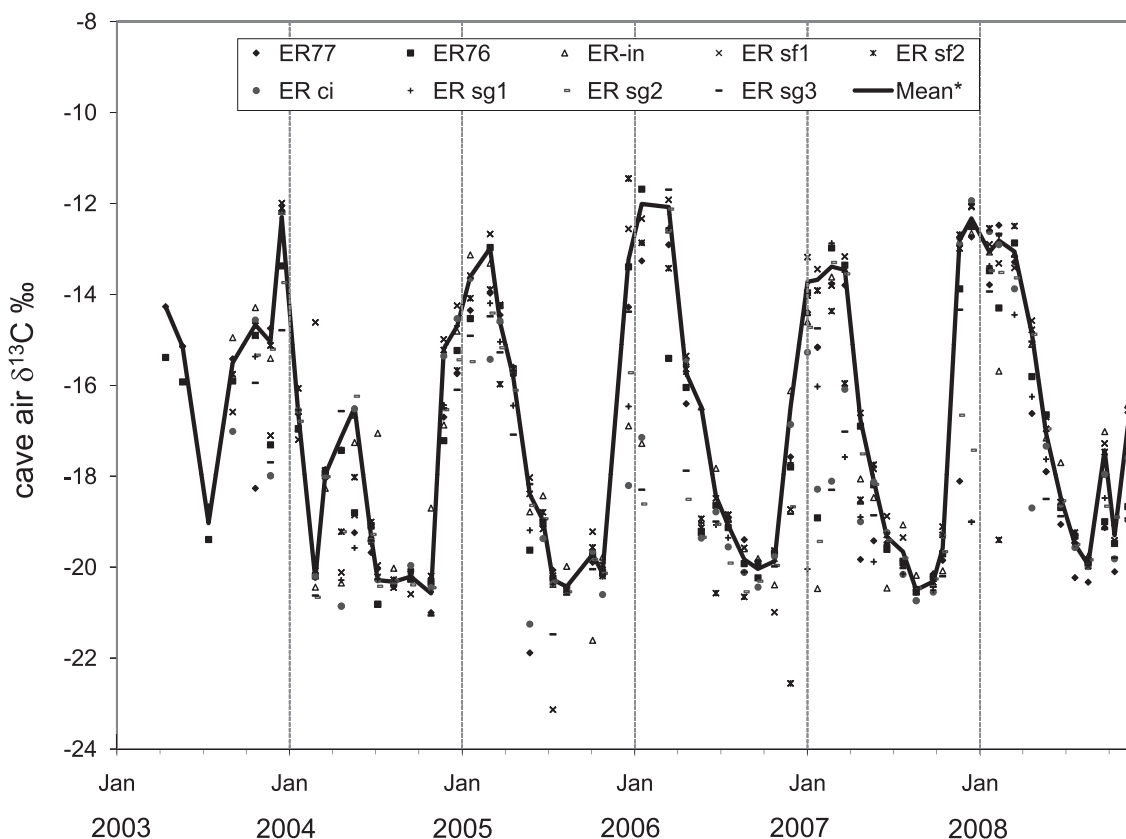


Fig. 5. Seasonal variability of $\delta^{13}\text{C}$ measured along the cave gallery showing a seasonal high in winter when pCO_2 is low. A total of seven sampling points were used and all display similar seasonal trends. A number of data points are anomalously low compared to other points in the same period of sampling and are suspected to have been contaminated by breath after the pCO_2 was measured (pCO_2 values vary little at any one time). The solid line represents the mean of values within 1‰ of the highest value measured at any one sampling episode. ER-in = entrance, ER sg1, 2 and 3 were collection points along the gallery, ER76 and ER 77 were collected in the deepest chamber.

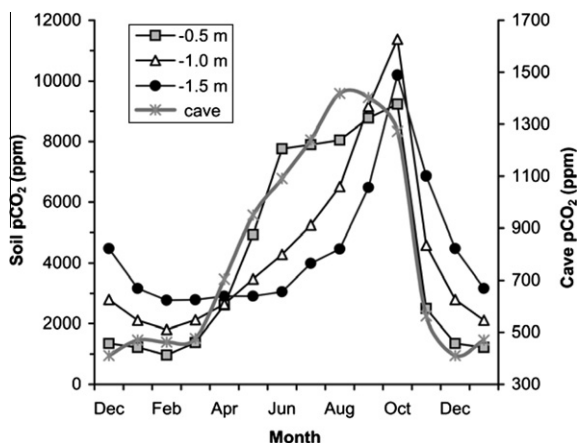


Fig. 6. Comparison between cave air pCO₂ and the soil air pCO₂ measured in the soil at 0.5, 1.0, and 1.5 m below the surface. Cave air roughly follows the trend of soil pCO₂ measured at 0.5 m, whereas the soil pCO₂ in the deeper samplers shows a delay of about two months in the maximum peak and also in the rapid autumnal decrease pCO₂ of the soil air.

The $\delta^{13}\text{C}_{\text{DIC}}$ values in the cave dripwaters are reported in Fig. 8 where the variability of soil water $\delta^{13}\text{C}_{\text{DIC}}$ values is also shown for comparison. The dripwater $\delta^{13}\text{C}_{\text{DIC}}$ values show a seasonal variability which roughly follows the soil water trend. Cave waters, however, are isotopically heavier (by 2–5‰) than soil waters. The highest isotope values pertain to the dripwater collected at the bottom of the cave from a low discharge, seepage drip (ER77) characterized by low discharge variability as indicated by the low (31%) relative standard deviation (Miorandi et al., 2010). The mean $\delta^{13}\text{C}_{\text{DIC}}$ for the dripwater collected at ER77 is -11.3‰ . The two drips sampled in Sala Grande (SG) at a depth of about -20 m show a ca. 1‰ difference in $\delta^{13}\text{C}_{\text{DIC}}$ between the fast discharge ER G1-st1 drip and

the slow discharge, seasonal drip ER76 (relative standard deviation of 94 and 81%, respectively). Overall, the mean $\delta^{13}\text{C}_{\text{DIC}}$ value for ERG1-st1 is -12‰ and for ER76, -11.4‰ . The drip with the highest relative standard deviation of discharge is, therefore, characterized by the most negative $\delta^{13}\text{C}_{\text{DIC}}$ values, whereas the more regular drip, with drip rates which change very little throughout the year, has more positive values. The cave dripwaters, regardless of the variation in discharge, are isotopically heavier with respect to the mean composition $\delta^{13}\text{C}_{\text{DIC}}$ of the aquifer water measured in the lysimeters (-14.5‰). The cave water $\delta^{13}\text{C}_{\text{DIC}}$ values also show a muted antipathetic trend with respect to cave air pCO₂.

The higher cave drip water $\delta^{13}\text{C}_{\text{DIC}}$ values compared to the deep soil waters, and the muted antipathetic trend with respect to cave air pCO₂ throughout the year point to: (1) host-rock dissolution en-route from the soil and upper epikarst to the cave, and/or (2) degassing modulated by the difference between seepage water and cave air pCO₂. In the first process we would expect an increase in dissolved Ca²⁺ concentration when dripwaters are characterized by higher $\delta^{13}\text{C}_{\text{DIC}}$ values. At Grotta di Ernesto, the dissolved Ca²⁺ concentration in the drips does not vary significantly between summer and winter (Frisia et al., 2003; Miorandi et al., 2010). In the following discussion we, therefore, test the hypothesis that degassing is an important process in the observed $^{13}\text{C}_{\text{DIC}}$ enrichment from the aquifer water to the cave drip sites.

5. DISCUSSION

5.1. Carbon dioxide fluxes

The seasonal change in the pCO₂ of cave air at Grotta di Ernesto is regarded primarily as a response to changing cave ventilation, rather than being modulated exclusively by soil conditions, primarily because the dripwater Ca²⁺

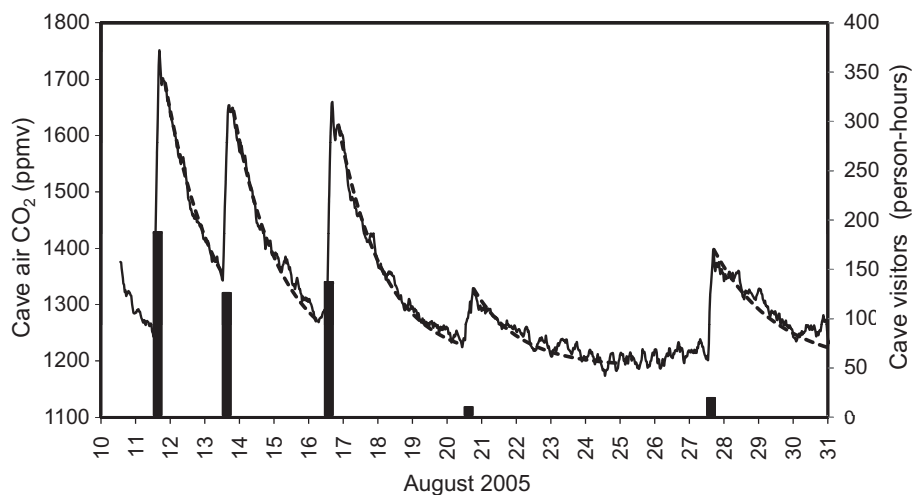


Fig. 7. Effects of visitors on cave air CO₂ concentration. The higher the number of visitors, the larger the increase in pCO₂ (used to estimate effective cave volume) followed by an exponential decline (used to estimate the air-exchange time with the exterior). The exponential models used are shown by the smooth lines overlying the data.

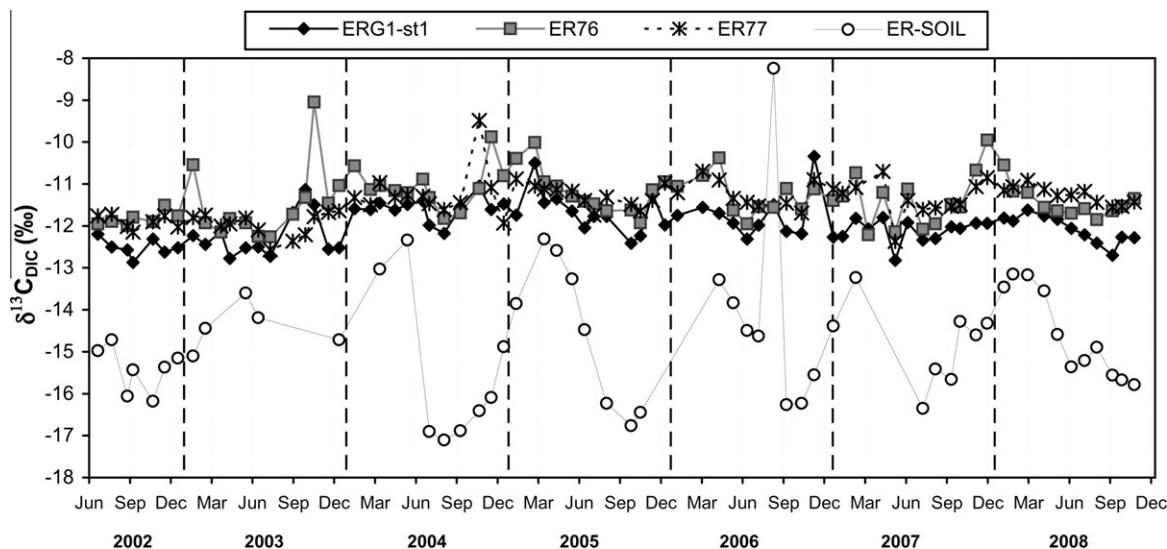


Fig. 8. Values of $\delta^{13}\text{C}_{\text{DIC}}$ (mostly HCO_3^-) in cave dripwaters compared with those in the soil water. ER76 is a low discharge seasonal drip, ER77 is a low discharge, seepage drip in the deepest part of the cave, and ER G1-st1 is a fast seasonal drip at the same level as ER76.

concentration is nearly constant throughout the year. This suggests that the epikarst supplying drip water has a year-round constant pCO_2 (Fairchild et al., 2000) and well-mixed seepage flow seepage flow drip (cf. Kluge et al., 2010). In addition, the change in cave air pCO_2 occurs rapidly and at precisely the time when the difference in temperature between interior and exterior reverses sign. This change in the difference between external and internal air temperature is a well-known key control on the intensity of cave ventilation by convection (Bourges et al., 2006).

Similar pCO_2 values in cave air measured in all parts of the cave suggest a uniform production and dispersion of carbon dioxide. At Grotta di Ernesto, biotic CO_2 production is negligible because of the absence of both active streams bringing into the cave organic matter from the outside, and bat colonies. Biotic CO_2 production, however, may be important in other caves and should be accounted for in the mass balance calculations. At Grotta di Ernesto, carbon dioxide fluxes can be quantified by using a mass-balance modelling approach. Fig. 9 illustrates carbon dioxide input to and output from the cave. When carbon dioxide levels are in steady-state (i.e. no climatic or anthropogenic transients) the CO_2 fluxes must balance:

$$F_1 + F_2 + F_3 = F_4 \quad (3)$$

F_1 refers to the daily input of CO_2 into the cave from the overlying soil and epikarst, which can be expressed as the product of V_1 , the daily input of gas (in litres) and C_1 , the carbon dioxide mass concentration per litre of air; F_2 is the daily mass input of CO_2 from degassing of dripwater; F_3 is the input of carbon dioxide from the external atmosphere ($= V_3 C_3$); F_4 is the output of carbon dioxide from the cave to the external atmosphere, which is equal to $V_4 C_4$ (where V_4 is set to be equal to V_3 for simplicity, an assumption justified by the subsequent analysis, and C_4 is the concentration of carbon dioxide in cave air). The role of cave biota is thought to be negligible at Grotta di Ernes-

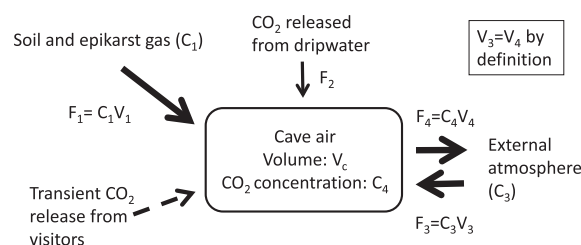


Fig. 9. Scheme of the gas-exchange model used to describe the regulation of the CO_2 concentration in the cave air of Grotta di Ernesto. Carbon dioxide flux (F , mass per unit time) is the product of the volume (V) of air being transferred per unit time and its concentration (C) of carbon dioxide. Quantification of the fluxes is discussed in the text (Section 5).

to and is not explicitly treated. In steady-state conditions, the cave concentration (C_4) becomes greater than that of the external atmosphere (C_3) (Faimon et al., 2006), thus:

$$C_4 = (F_1 + F_2) / V_4 + C_3 \quad (4)$$

The presence of visitors provides a short-term injection of CO_2 leading to a transient increase of the cave air CO_2 level, which then declines exponentially over a period of a few days (Fig. 7). This allows summer values of F_3 and F_4 to be estimated (Table 2). The number of visitors is known and the duration of their visits is approximately known. Most visitors are primary-school children whose CO_2 production is roughly half that of an adult (Kivastik, 1998). The increase in CO_2 in ppm per adult-equivalent person-hour in the cave (R), calculated from the data presented in Fig. 7, varies from 5.6 to 28, a large range which probably reflects uncertainties in estimating the duration of visits and possibly different proportions of time spent in different parts of the cave. To weight each data-point equally, the median value of R (13.6 ppm/person-hour) is taken as representative. Given that adult human respiration produces

Table 2

Summary of the mass fluxes (kg day^{-1}) and air-exchange times in different seasons. Three mass-balance models are calculated for winter (winter models 1, 2, and 3) and are discussed in the text. F_1 is the daily input of CO_2 from the soil, F_2 is the daily CO_2 evolved from degassing, F_3 is CO_2 contribution to cave air from the external atmosphere, and F_4 (the sum of F_1 , F_2 and F_3) is the CO_2 flux from the cave to the exterior.

	F_1	F_2	F_3	F_4	Air-exchange time (days)
Summer 2005	1.58	0.03	0.73	2.34	1.43 (observed)
November 2008	1.44	0.05	2.45	3.93	0.43 (observed)
Winter model 1 (same V_3 as November)	0.30 (10.7%)	0.06 (2.1%)	2.44 (87.2%)	2.80	0.43 (model)
Winter model 2 (same F_1 as November)	1.44 (12.3%)	0.06 (0.5%)	10.21 (87.2%)	11.71	0.10 (model)
Winter model 3 (constrained by carbon isotope data)	(12.5%)	(2%)	(85.5%)		Not specified

480 litres of exhaled breath per hour (Kivastik, 1998) with a concentration (C_b) of 36000 ppm CO_2 , and assuming an equal dispersion throughout the cave volume, the effective cave volume (V_c) in litres can be calculated:

$$V_c = (480/R)(C_b - C_4) \quad (5)$$

The estimated V_c (1.3×10^6 l) is within 30% of the first-order estimated cylindrical volume of Grotta di Ernesto. The propagated uncertainty in parameter R will not affect relative comparisons between winter and summer conditions.

The observed exponential decline in the excess CO_2 concentration in the cave air is expected from the regulating effect of exchange of equal volumes of air between the interior and the atmosphere in the box model. Hence:

$$C_t = C_i e^{-\lambda t} \quad (6)$$

where C_t is the cave air concentration of CO_2 above the background level at time t after the visitors have left, C_i is the initial peak value above background and λ is the decay constant. The relaxation time $1/\lambda$ corresponds to the exchange time of the cave air. Eq. (6) has been solved by curve-fitting using an estimated error of less than $\pm 10\%$ on t arising from minor uncertainties in determining the background level and specifying the onset of the exponential decline. The mean values for one event in June and five events in August is 1.43 ± 0.3 days. This value determines the daily rate of air exchange V_3 ($=V_4$) and the equivalent large fluxes F_3 and F_4 can hence be calculated as shown in Table 2.

F_2 refers to the carbon dioxide released by degassing of incoming water which is commonly regarded as a major carbon dioxide source to caves. However, at Grotta di Ernesto, this flux is found to be small; because this was not initially expected, it has been estimated by three different methods for confirmation. The carbon dioxide released can be readily calculated by the difference in total inorganic carbon between undegassed water entering the cave and water that has equilibrated with cave air and so the key uncertainty is water flux. The first approach to estimate mean water flux is by calculating how much water infiltrates within the horizontal outline of the cave, given a precipitation minus evaporation value of 500 mm/year. This results in 2.5×10^5 l of dripwater per year and a CO_2 efflux of between 0.03 and 0.05 kg day^{-1} in summer and winter, respectively (Table 2), which is small in comparison to F_3 . The second method cumulates the water entering from drips that are being monitored and makes an estimate of the

water influx at the other drip points that are not being monitored. This is a semi-quantitative approach (within an order of magnitude), but results in values only 20% as large as those calculated with the first method. Thirdly, direct evidence of CO_2 efflux from degassing was provided by a transient rise in carbon dioxide accompanying a hydrological event on 24–25 November 2007 (data plotted in Miorandi et al., 2010) which was continuously monitored at two low-discharge drips with different characteristic variabilities in drip rate (one high and the other one low). Before the event, discharge of both drips was close to the mean of the period 2003–2007, whilst cave air CO_2 concentration was around 400 ppm. A 24-h peak averaging five times the preceding discharge in both drips quickly dropped to twice the normal value. Correspondingly, CO_2 rose by 250 ppm followed by a rapid drop to <100 ppm above the background level, all within a few hours. Assuming that a CO_2 anomaly from water efflux is diffused through the cave in the same way as CO_2 introduced from human activity, the transient rise in CO_2 corresponds to an additional emission of only 0.005–0.01 kg (less than the minimum daily values used for F_2 in Table 2), and even this small figure may include a proportion of gas expelled from karst cavities, as the aquifer fills during the hydrological event. In essence, it is apparent that in steady-state the CO_2 efflux from dripwater has only a small effect on the carbon dioxide mass balance at this site.

Eq. (3) can now be solved for summer conditions and F_1 is 1.58 kg day^{-1} . Evidently there is a large flux of soil-derived CO_2 into the cave, as inferred by Ek and Gewelt (1985), who were able to demonstrate increasing CO_2 levels through fissures in the roof of a shallow Belgian cave.

A key issue is to understand how the system behaves in winter when carbon dioxide levels in the cave are effectively held at levels only 15% higher than those of the external atmosphere. A CO_2 -release experiment conducted at the end of the monitoring period in November 2008 during the transition to the low- CO_2 winter regime illustrates some features of the dynamics of air circulation. After careful calculation that the mass of CO_2 to be released within the cave would not cause a health hazard, a carbon dioxide cylinder was emptied by uniformly releasing the gas throughout the cave, and the decay in CO_2 concentration was measured at two locations – one in Sala Terminale, as in previous periods of logging, and a second location higher up in Sala Grande. The peak concentration of 2800 ppm in Sala Grande at the end of the release decayed exponentially yielding an air-exchange time of 0.43 days. Circulation

was rapid and the concentration stabilized at 700 ppm in less than three days. The concentration at Sala Terminale was 4500 ppm and the first four hours of decay fit the 0.43 day exchange pattern, but over the next three days the decline was quasi-linear and slower than expected, followed by a fairly abrupt stabilization at 1600 ppm after 4 days. Hence, zonation had developed and the quasi-linear decline suggests diffusive rather than turbulent mixing phenomena. The lack of a vertical carbon dioxide gradient during previous observations implies that the rapid decline in Sala Grande can be tentatively taken to reflect the overall pattern of circulation. If so, then the solution of Eq. (5) for a 0.43 day exchange time suggests that V_3 increased significantly compared to summer (Table 2), which can be attributed to stronger downward convection of cold air in winter.

When the winter mode is fully developed, $p\text{CO}_2$ levels are held at around 500 ppm and this low carbon dioxide level could reflect either a shorter air-exchange time or a reduction in the flux from the soil and epikarst (F_1), or both. The air-exchange time could not be determined because the cave could not be accessed in winter, but two end-member model solutions are provided. In model 1 (moderate ventilation model) the air-exchange time is kept the same as in November 2008 (3.4 times higher than in summer); this would require a strong decrease in F_1 . In model 2 (high ventilation model), F_1 is kept constant, but a much faster air-exchange is now required, 14 times higher than in summer. Both ratios of summer-to-winter exchange times fall within the range of values recalculated from literature, and values based on radon data in caves (e.g. Hakl et al., 1997). $\delta^{13}\text{C}$ data provide additional insight into the air exchange mechanisms, as discussed in Section 5.3.

5.2. Roles of advection and diffusion in CO_2 fluxes

The mass-balance model has been constructed in terms of air advection between the cave and the outside atmosphere. The potential role of diffusion is also considered because fractionation of carbon isotopes occurs during this process (e.g. Cerling et al., 1993).

Given that the cave entrance is sealed by a solid door and there are no obvious large fractures or cavities connecting the underground passages to the external atmosphere, ventilation of the cave must take place via narrow fissures and/or pores. Neglecting frictional drag, we can characterize these small cavities collectively in terms of their mean length (L) between the cave and Earth's surface and the total cross-sectional area (A) perpendicular to L .

The advective flux (F_{adv} in $\text{mg cm}^{-2} \text{sec}^{-1}$) can be defined in terms of the product of concentration (C) and velocity of air flow (U)

$$F_{\text{adv}} = C \cdot U \quad (7a)$$

The mean CO_2 concentration ($0.00123 \text{ mg cm}^{-3} = 650 \text{ ppm}$) is represented by the difference in concentrations between the outflowing air and the inflowing atmospheric air (0.00188 and $0.00065 \text{ mg cm}^{-3}$, i.e. 1190 and 520 ppm, respectively):

$$F_{\text{adv}} = 0.00123 \cdot U \quad (7b)$$

A diffusional flux (F_{diff}) in still air, with the net effect of causing the migration of gas down a concentration gradient, is expressed as:

$$F_{\text{diff}} = D \cdot dC/dx \quad (8a)$$

where D is the diffusion coefficient in air ($0.14 \text{ cm}^2 \text{ sec}^{-1}$ for CO_2 , see Bourges et al., 2006) and dC/dx is the concentration gradient, with the distance dx corresponding to the length L . dC has the same value as C in Eq. (7) and so Eq. (8a) becomes:

$$F_{\text{diff}} = 0.14 \times 0.00123/L = 1.72 \times 10^{-4}/L \quad (8b)$$

The mass balance model indicates that the net movement of CO_2 out of the cave in summer is $2.3 \times 10^6 \text{ mg day}^{-1}$ ($= 27.1 \text{ mg sec}^{-1}$); alternatively it can be expressed as an observed flux (F_{obs}) per unit area (A):

$$F_{\text{obs}} = 27.1/A \quad (9)$$

Hence for advection, combining (7b) and (9):

$$U \cdot A = 22033 \quad (10)$$

And for diffusion, combining (8b) and (9):

$$L/A = 6.4 \times 10^{-6} \quad (11)$$

The calculated advective and diffusive flows required to describe air exchange at Grotta di Ernesto are shown graphically in Fig. 10. Diffusion becomes ineffective over longer path-lengths, but the geometry of the cave system is such that the path-length L must be at least 1 m. Under those conditions, the area A must be $\geq 10^7 \text{ cm}^2$, which can be ruled out based on the lack of visible openings to the outside. For advection, the constraint is that no air currents were detected, hence V must be $< 1 \text{ cm sec}^{-1}$. A range of feasible solutions is shown by Fig. 10 where undetectably slow air movement along openings with aggregated areas in the range 2×10^4 to $2 \times 10^5 \text{ cm}^2$ can account for the ventilation of the cave. Under winter conditions, the required air exchange is faster and diffusion is even less likely since the difference in concentration between the cave and outside atmosphere is small. In summary, the flux of CO_2 from the cave can be treated almost exclusively as advection, where strong seasonal differences in flow rates most probably induced by temperature differences occur between the surface and the cave atmosphere, which force the flow of gas with differing densities in and out of the cave (see Bourges et al., 2006).

5.3. C isotope mass-balance model

Carbon isotope ratios of cave drip water DIC are higher than in soil water (Fig. 11). This could be attributed to the loss of isotopically light CO_2 during the degassing process. Dulinski and Rozanski (1990) constructed a semi-dynamic model which predicted a strong kinetic fractionation related to a one-way mass transport accompanying water degassing in the cave, but their theoretical model needs to be tested using observational evidence. The occurrence of strong kinetic effects during degassing was demonstrated at Obir cave in Austria, a system which is characterized by a large-scale chimney-type circulation sustained by the

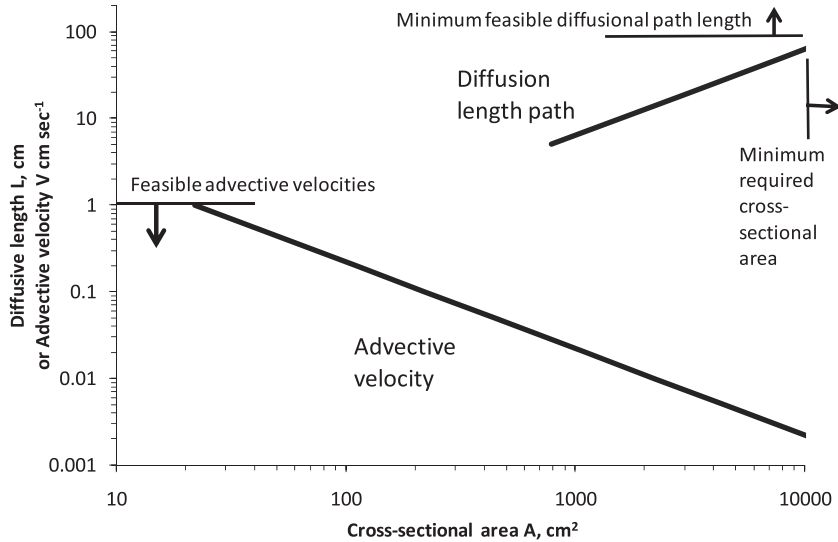


Fig. 10. Calculated characteristics of advective and diffusive flows required for ventilation at Grotta di Ernesto in the warm season. Cross-section areas and length of cave passages required for diffusion are inconsistent with the geometry of the cave. Advection is considered the key process responsible for cave ventilation (see text for details).

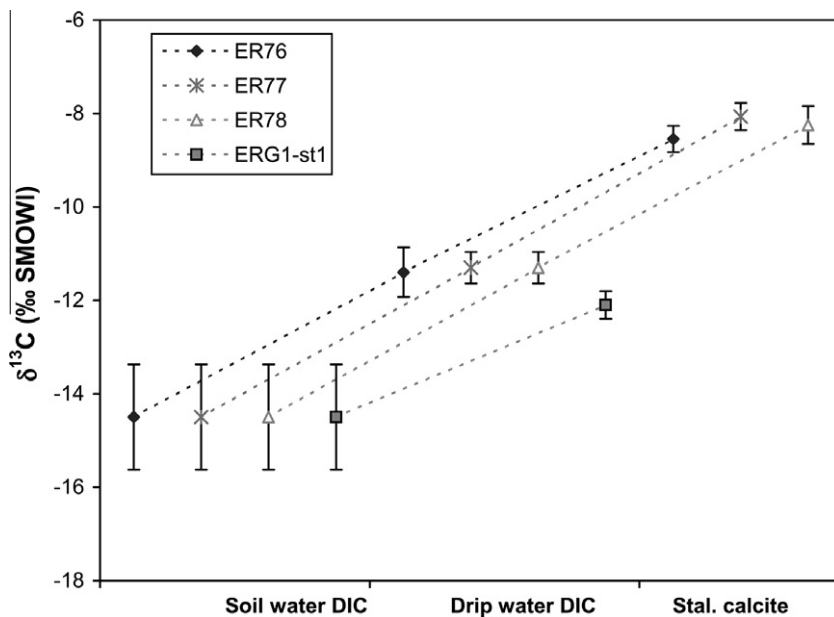


Fig. 11. The $\delta^{13}\text{C}_{\text{DIC}}$ values of soil waters, drip waters and $\delta^{13}\text{C}_c$ of stalagmite calcite (top 10 mm representing the last ca. 20 years) for ER-76, 77, 78 and ER G1 st-1 fast-dripping site. The fast ER-st1 (G1) drip feeds a large flowstone with ridges and furrows, which we chose not to sample as it may have been affected by dissolution in the summer season.

difference in external and internal air density (Spötl et al., 2005). At Grotta di Ernesto, advection drives CO_2 fluxes, with the pCO_2 gradient between dripwater and cave air being higher in winter, a difference that can be attributed to enhanced convection of cold air from the exterior into the descending cave cavity (cf. Bourges et al., 2006). The active air circulation would tend to promote kinetically enhanced degassing. Building on and extending the approach of Spötl et al. (2005), we can test for the occurrence of kinetic fractionation during the initial phase of degassing (Dulinski and Rozanski, 1990).

The carbon isotopic composition of cave air in Grotta di Ernesto can be described in terms of a combination of end-members in a three-component mixing model. End-member 1 corresponds to the composition of soil and epikarst air, which is here taken as the mean annual composition of soil gas measured at 1.5 m depth ($\delta^{13}\text{C} = -23.1\text{‰}$ and 4950 ppm CO_2). This lies just above the continuation of the trend displayed by the summer cave air samples (Figs. 12 and 13). End-member 2 corresponds to the composition of the CO_2 which entirely evolves from fast degassing and slow equilibration into the cave air. Qualitatively, this must

be isotopically light and in the next section we justify an estimate of -70‰ for its $\delta^{13}\text{C}$ value. End-member 3 is the external air under the forest canopy. The $p\text{CO}_2$ of the forest air in the area is well-constrained by measurements (Marcolla et al., 2005), consistent with the mean of measurements during an annual cycle in the present study of around 440 ppm; its isotopic composition, however, has not been directly determined. We calculated the $\delta^{13}\text{C}$ composition of end-member three by adding sufficient carbon dioxide generated by respiration of a C_3 plant assemblage ($\delta^{13}\text{C} = -25\text{‰}$) to the composition of clean atmosphere (382 ppm and -8.1‰ as measured in Hawaii (NOAA website), to attain the measured composition of 440 ppm CO_2 which yields a $\delta^{13}\text{C}$ composition of -10.2‰ .

The mass balance results from the carbon dioxide flux model presented in Table 2, are plotted in Figs. 12 and 13, and show a good correspondence with the independent constraints of $\delta^{13}\text{C}$ data. Winter model 1 (moderate ventilation) lies closer to the cluster of winter air data than does winter model 2 (strong ventilation), which has a lower contribution from CO_2 -degassing because of the higher total C fluxes. A model tuned to the carbon isotope data (Model 3) corresponds to a three-component mixture that is centred within the measured cluster of winter data (Figs. 12 and 13). This air has a similar (2%) proportion of degassed CO_2 in the total carbon budget as model 1, but a slightly different ratio of epikarst air to external atmosphere contribution. Overall, the agreement between modelled and real cave air composition is very close and the contribution derived from air-water interactions (corresponding to F_2 in Section 5.1), although small, is clearly quantifiable using the isotope data. The better-fit of model 1 with the measured data compared to model 2 has implications for the winter mass balance, as it indicates that there is a significant decrease in the CO_2 supply (from 1.44 to 0.30 kg day^{-1})

from the epikarst compared with the transitional period in November 2008. This may be explained by blockage of airways such as thin fractures and pores by water, following an increase in hydrological infiltration as has been demonstrated at Castañar de Ibor, a cave in Spain, by Fernandez-Cortes et al. (2009).

5.4. Mass balance constraints on the carbon isotope evolution from the soil to the stalactite

At Grotta di Ernesto soil water collected in two lysimeters shows variations in $\delta^{13}\text{C}$ values that roughly parallel those of the soil gas, with a mean difference of $8.6 \pm 1.0\text{‰}$. The lysimeter waters yielded similar mean $\delta^{13}\text{C}$ values (-14.4‰ and -14.7‰), which are slightly lower than expected from equilibration with mean soil gas with a mean C isotope composition of -23.1‰ at 4950 ppm CO_2 ($p\text{CO}_2 = 10^{-2.3}$; soil gas $\delta^{13}\text{C}$ values vary between -21 and -25‰). A mean $\delta^{13}\text{C}$ value of -14.5‰ for the soil water is used here in the geochemical calculations.

Modelling of the $\delta^{13}\text{C}$ evolution focussed on the cave dripwater in order to ensure consistency when comparing modelled and measured DIC concentrations in the soil. Dripwater $\delta^{13}\text{C}_{\text{DIC}}$ shows only muted annual variability, because it is derived from epikarst water which equilibrated with the mean soil gas composition; in addition, there is no evidence of prior calcite precipitation (which would affect the C isotopic composition of dripwater (Fairchild et al., 2000; Fairchild et al., 2006b). Dripwater was collected within a few minutes, so these samples had not yet completely degassed (data from the 1994–1997 field campaign shows that drips in Sala Grande collected in a similar way had pH values several tenths of a pH unit below those that would correspond to equilibration with cave air). Results reported in Section 4.2 indicate that the $\delta^{13}\text{C}_{\text{DIC}}$ values of

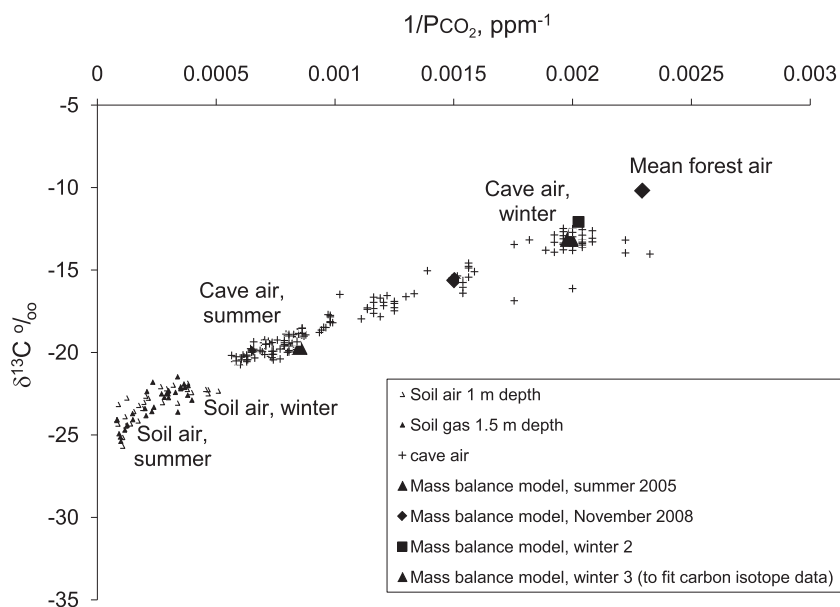


Fig. 12. $\delta^{13}\text{C}$ composition and $p\text{CO}_2$ of soil air and cave air compared with points calculated from the mass-balance models (see text for details). Suspected contaminated samples of cave air have been omitted.

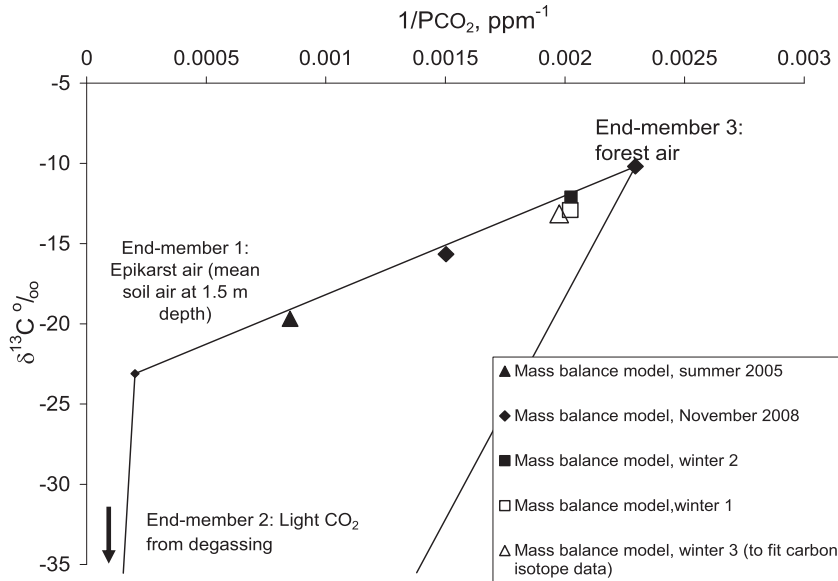
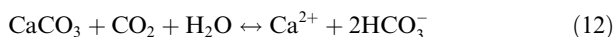


Fig. 13. End-member isotopic mixing model in relation to values calculated from mass-balance modelling independent of the isotopic composition. The moderate ventilation model “winter 1” is more consistent with the isotope data than the high-ventilation “model 2”.

dripwater entering the cave are significantly higher (2.5‰ for the fast drip and about 3‰ for the slow drips) than the mean values of soil waters (Fig. 11), although the trends of seasonal variability are similar (Fig. 8). This enrichment can be explained by two processes, one occurring in the aquifer and the second in the cave.

The first process is the dissolution of carbonates in the soil and in the aquifer zones. Soil water has variable Ca²⁺ concentrations, but its mean value lies below the Ca²⁺ concentration measured in the dripwater for the fast stalactite ER G1 st-1 drip (59 mg/l), indicating that additional Ca²⁺ must be provided by the dissolution of carbonates in the regolith and host rock (Fohlmeister et al., 2010). The mean soil air pCO₂ is about 5000 ppm (Miorandi et al., 2010), which is in equilibrium with the soil water, and is higher than the calculated pCO₂ in equilibrium with the dripwater before degassing (Table 3). The mean dripwater composition at three drip sites characterized by fast seasonal discharge (ER G1 st-1), low seasonal discharge (ER76), and low seepage discharge (ER77) shows pCO₂ values between 10^{-2.8} and 10^{-2.9} (1250–1600 ppm). Using the program MIX4 (Fairchild et al., 2000), these values were back-tracked by adding CO₂ to restore them to being just saturated with respect to calcite: this is the second set of results in Table 3. The pCO₂ values obtained at calcite saturation are slightly below the mean value of the soil waters (10^{-2.3} = 5000 ppm). The decrease in pCO₂ from the soil to the back-tracked waters that are the source waters of the cave drips is likely to be related to carbonate acid hydrolysis, when little or no soil CO₂ is added to the solution according to the reaction:



This means that the extra Ca²⁺ measured in the dripwater is due to carbonate dissolution in a closed system (Hendy, 1971). Radiocarbon activity in the dripwater

allows us to quantify the host rock contribution to the total dissolved inorganic carbon budget. We assume a radiocarbon activity for the soil gas on the order of 110 pmC, which was calculated by using the model proposed by Genty and Massault (1999) and the bomb peak recorded in Grotta di Ernesto stalagmites (Fohlmeister et al., in press). The dripwater mean ¹⁴C activity is 99 pmC (Fohlmeister et al., 2010). This supports contribution from the host rock to the total DIC in the order of 10%. We then would expect enrichment in ¹³C of the dripwater DIC of about 1.5‰ related to carbonate dissolution prior to any process occurring in the cave.

The second process is degassing of the initial solution of the system H₂O–CO₂–CaCO₃ upon coming into contact with the cave atmosphere. This process is assumed to occur relatively rapidly, driven by a sharp concentration gradient at the boundary between the surface of the drop and the atmosphere (Dreybrodt, 2008). The measured dripwater was degassed using the program MIX4 until it attained a pCO₂ of 10^{-3.3} (500 ppm), which is a typical concentration of winter cave air in Grotta di Ernesto. These are the set of results reported in the third row in Table 3. The isotopically light CO₂ evolved from the dripwater must then become mixed within the cave air and corresponds to end-member 2 in Fig. 13.

5.5. Carbon isotope exchanges in the solution film on the stalagmite

In the previous Section 5.4, we considered the evolution of the δ¹³C_{DIC} values prior to reaching the cave due to water-rock interactions and an initial first phase of degassing, which occurs prior to the formation of a solution film on the top of the stalagmite, based on monitoring data. The exact rate of degassing in this initial phase is unknown, because the configuration of the water/air interface is

Table 3

Measured and modelled water compositions used for mass-balance calculations. For the sake of simplicity a completely degassed water (during winter conditions) is assumed in the mass-balance model, although complete degassing is probably unlikely to occur in nature.

	ERG1 st-1	ER76	ER77
<i>Mean measured composition of dripwater (2007–2008)</i>			
pH	8.02	8.07	8.07
DIC (mg L ⁻¹)	201.9	194.3	197.3
pCO ₂	10 ^{-2.83}	10 ^{-2.90}	10 ^{-2.89}
ppm	1480	1260	1290
<i>Modelled composition at calcite saturation before degassing</i>			
pH	7.65	7.66	7.66
DIC (mg L ⁻¹)	210.2	202.6	205.8
pCO ₂	10 ^{-2.45}	10 ^{-2.49}	10 ^{-2.47}
ppm	3550	3240	3390
<i>Modelled composition (completely degassed) in winter cave pCO₂ condition of 10^{-3.3} (500 ppm)</i>			
pH	8.48	8.46	8.47
DIC (mg L ⁻¹)	195.85	189.35	192.2

variable. Some initial degassing may occur above the cave ceiling when an air-water interface first develops and will continue as the water migrates. Our observations and models, however, critically indicate that the first phase of degassing is an irreversible reaction and, consequently, isotopic fractionation is dominated by kinetics rather than equilibrium. This, however, is only part of the picture when comparing the $\delta^{13}\text{C}_{\text{DIC}}$ values of dripwaters with the $\delta^{13}\text{C}$ values of modern carbonates (sampled at speleothems active at the time of collection) in Grotta di Ernesto, which range from mean values of approximately $-8\text{‰} \pm 1\text{‰}$ in soda straws (hollow stalactites), of about $-7.5\text{‰} \pm 1\text{‰}$ in stalagmite calcite, and approximately -5‰ in cone stalactites, spray and wall deposits. The $\delta^{13}\text{C}$ values of calcites precipitated during the last 20 years and deposited at the impact point at the tip of stalagmites ER76, 77 and 78 are all ca. -8‰ . These values are higher than expected for equilibrium deposition from dripwaters with $\delta^{13}\text{C}$ values of about -11‰ (Fig. 11), because there is negligible C-isotope fractionation between DIC and CaCO_3 at the ambient cave temperature. Hence, at Grotta di Ernesto, mass-balance modelling of C isotope composition evolution must explain the progressive kinetic enrichment from the soil water to the speleothems.

At Grotta di Ernesto, a kinetic enrichment occurs in the parent solution due to the preferential escape of isotopically light CO_2 from the fluid to the air even before calcite deposition commences on the top of the stalagmite. The mass-balance models we used to describe CO_2 fluxes at Grotta di Ernesto, in fact, require a small percentage of ^{13}C -depleted carbon dioxide to explain the displacement of the measured cave air C-isotope values from the mixing line which represents varying proportions of mixing between the pure soil-air and the mean forest air end members.

Degassing of CO_2 shifts the carbonate equilibrium toward supersaturation and leads to calcite precipitation at near-neutral pH. During this reaction, approximately one mole of CO_2 is slowly released for each mole of CaCO_3 (Dreybrodt, 2008; Scholz et al., 2009). Isotopic fractionation during calcite precipitation is regarded as kinetically influenced (Dreybrodt, 2008) as precipitation can only occur in solutions with a certain degree of supersaturation.

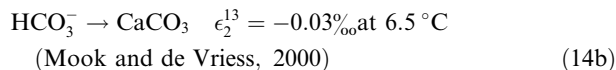
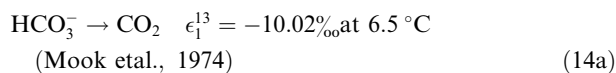
Nevertheless, calculations of the C-isotope evolution during calcite formation commonly assume isotopic equilibrium because the kinetic effects are not quantitatively known (Dreybrodt, 2008). Consequently, we assume that calcite precipitation in Grotta di Ernesto also occurs close to isotopic equilibrium and for the purpose of calculating mass balance we assign all ^{13}C -enrichment beyond the constraints of the calcite precipitation reaction to the other two processes, i.e. fast degassing of water towards the limiting pCO₂ of cave air, and slow equilibration of aqueous and gaseous species.

The third step is the progressive equilibration between the solution and the cave atmosphere, which can be represented as the exchange reaction



This process is assumed to take over from kinetic degassing once the pCO₂ of the dripwater approximates that of the cave air (Hendy, 1971; Scholz et al., 2009). In the circumstance where the dripwater DIC has carbon isotope compositions less than 9.7‰ higher than the C isotope composition of the cave air, and for a temperature of less than 10 °C (which is the case in Grotta di Ernesto), modelling has shown that equilibration results in the dripwater evolving to higher $\delta^{13}\text{C}_{\text{DIC}}$ values (Scholz et al., 2009).

We follow Mühlinghaus et al. (2009) and Scholz et al. (2009) in using the following values of equilibrium fractionation factors for the isotopic exchange between bicarbonate in the solution film present on top of stalagmites and carbon dioxide in the cave atmosphere, and bicarbonate in the solution film and calcite:



Note that ϵ_2^{13} is zero within analytical error, so we assume no fractionation between dissolved inorganic carbon (dominantly bicarbonate) and CaCO_3 . We used the set of data reported in Table 3 to perform the calculation of the $\delta^{13}\text{C}$ of the light end member (2) derived from the

mass-balance model. In Table 4 we report the calculated mass balance for carbon isotopes for the measured and modelled water composition presented in Table 3. The mass balance calculation has been based on the change in total dissolved inorganic carbon:

$$\begin{aligned} \text{DIC}_i &= [(\text{CO}_3^{2-}) + (\text{HCO}_3^-) + (\text{CO}_{2\text{aq}}^*)]_i \\ &= [(\text{CO}_3^{2-}) + (\text{HCO}_3^-) + (\text{H}_2\text{CO}_3^*)]_{\text{dripwater}} \\ &\quad + (\text{CO}_2)_{\text{degassed}} \end{aligned} \quad (15)$$

where the parentheses () indicate concentrations, and i is used to indicate the initial water composition prior to degassing.

At the pH values measured and calculated for the waters in the soil-cave system, $(\text{HCO}_3^-) \gg (\text{CO}_3^{2-}) + (\text{CO}_{2\text{aq}}^*)$ and the $\delta^{13}\text{C}$ of $\text{TDIC} \approx \delta^{13}\text{C}$ of HCO_3^- .

Hence the mass-balance equation is:

$$\begin{aligned} \text{DIC}_k \delta^{13}\text{C}_k &= \text{DIC}_{\text{dripwater}} \delta^{13}\text{C}_{\text{dripwater}} \\ &\quad + [\text{CO}_2] \delta^{13}\text{C}_{\text{degassed CO}_2} \end{aligned} \quad (16)$$

where $[\text{CO}_2]$ refers to the mass of CO_2 removed per litre of solution and k refers to the lower soil and upper epikarst.

In the following discussions, the row numbers referred to are those of the rows in Table 4. We assume that the aquifer water $\delta^{13}\text{C}_{\text{DIC}}$ value is equal to that measured in soil water modified by the contribution from host rock dissolution and characterized each drip through their mean dripwater $\delta^{13}\text{C}$ composition (row 1). The CO_2 degassed from the solution was calculated using Eq. (16) to have a composition of -34.9‰ for the fast drip ER G1 st-1 and a composition of -50.5 to -52.5‰ for slower drips ER76 and ER77 (row 2). Consequently, the degassed CO_2 is

kinetically fractionated, because equilibrium fractionation would have resulted in the loss of CO_2 with $\delta^{13}\text{C}$ no more negative than -24.5‰ (Mook et al., 1974; Mook, 2006). The modern calcite formed on stalagmites ER76 and ER77 is isotopically heavier than the dripwater collected at the respective feeding stalactites (row 3), requiring a total $\delta^{13}\text{C}$ change in the order of about 4.7‰ (row 4; note that the flowstone beneath drip ER G1 st-1 was not sampled as its irregular surface morphology makes it doubtful that modern equilibrium precipitates are present). This implies that, by comparing initial water and stalagmite water, the isotopic composition of the CO_2 degassed from dripwater is even lighter than that calculated by using Eq. (16) for the $\delta^{13}\text{C}$ of the degassed CO_2 evolved at the initial stage of degassing (compare rows 5 and 2). If the CO_2 lost from the solution by the degassing process continued to have the $\delta^{13}\text{C}$ values calculated in row 2 whilst degassing continued to the winter pCO_2 of $10^{-3.3}$, then the resulting stalagmite calcite $\delta^{13}\text{C}$ values would be those reported in row 6. The total isotopic change attributable to degassing is given in row 7, and the remaining discrepancy to the stalagmite C isotopic composition which would be attained by equilibration with the cave atmosphere is given in row 8. Then, the total proportion of ^{13}C enrichment to the $\delta^{13}\text{C}$ values of stalagmite calcite attributable to degassing is 58 and 57% for ER76 and ER77, respectively (row 9). Most of this enrichment is accounted for by kinetically enhanced degassing. If we consider that the additional rise in $\delta^{13}\text{C}$ values was due to partial exchange equilibration with a large air reservoir of fixed composition (Scholz et al., 2009), we can compare the C isotope composition with that of the expected end-point of such equilibration, which is -3‰ , about 10% heavier than the cave air (rows 10 and 11). For drips

Table 4

Mass-balance calculations of $\delta^{13}\text{C}$ composition of CO_2 lost from solution during evolution of water at Grotta di Ernesto. See text for discussion. The absence of prior calcite precipitation at Grotta di Ernesto implies that the degassed dripping water C isotopic composition is directly reflected by the C isotopic composition of speleothem calcite. Since the C isotopic fractionation between HCO_3^- and CaCO_3 at 6.5 °C (the cave temperature is 6.7 °C) is approximately zero (Mook and De Vriess, 2000), and the typical value of calcite at the top of modern stalagmites in this cave is -8.1‰ , we infer that this is the value of dripwater at the splashing point.

	ER G1st-1	ER76	ER77
1. Mean $\delta^{13}\text{C}$ composition of dripwater (at the top of the stalagmite)	-12.1‰	-11.4‰	-11.3‰
2. $\delta^{13}\text{C}_{\text{degassedCO}_2}$ (comparing initial water and dripwater, note that the initial water is taken as -13‰)	-34.9‰	-50.5‰	-52.5‰
3. Mean $\delta^{13}\text{C}$ composition of stalagmite and DIC from which it formed	n/a	-8.54‰	-8.07‰
4. $\delta^{13}\text{C}$ change from initial to final water		$-13\text{‰} - (-8.54\text{‰}) = -4.46\text{‰}$	$-13\text{‰} - (-8.07\text{‰}) = -4.93\text{‰}$
5. $\delta^{13}\text{C}_{\text{degassedCO}_2}$ (comparing initial water and stalagmite water)	n/a	-76.7‰	-82.7‰
6. Expected stalagmite composition if CO_2 were lost with composition as in 2.	-11.4‰	-10.4‰	-10.2‰
7. $\delta^{13}\text{C}$ change attributed to degassing		$(-13\text{‰} - (-10.4\text{‰})) = 2.6\text{‰}$	$(-13\text{‰} - (-10.2\text{‰})) = 2.8\text{‰}$
8. Difference in stalagmite composition attributed to equilibration		$(-8.54\text{‰} - (-10.4\text{‰})) = 1.86\text{‰}$	$(-8.07\text{‰} - (-10.2\text{‰})) = 2.13\text{‰}$
9. Proportion of stalagmite ^{13}C -enrichment attributed to degassing		$2.6/4.46 = 58\%$	$2.8/4.93 = 57\%$
10. Cave air composition in winter		-13‰	-13‰
11. Expected water and stalagmite composition if controlled by equilibration with cave air in winter		-3‰	-3‰
12. Proportion of maximum potential equilibration observed		$1.86/(10.4 - 3) = 25\%$	$2.13/(10.2 - 3) = 30\%$

ER76 and 77, respectively, we found (row 12) that the waters have achieved 25% and 30%, respectively of the potential equilibration with cave air.

Overall a $\delta^{13}\text{C}$ value of ca. -76‰ is representative of the total degassed CO_2 derived from the first rapid phase at tip of the stalactite and the second phase at the splashing site for ER76 and ER77. In calculating end-member 2 in Section 5.3 however, we adopted the slightly higher value of -70‰ . The reason for doing this is that this end-member reflects the mean C isotopic composition of carbon dioxide leaving water in the cave as a whole. A significant proportion of the total carbon dioxide pool degassed from dripwaters arises from a few fast drips such as ER G1st-1, which was found to have released CO_2 that was significantly heavier, by 16–18‰ than ER76 and ER77 (line 2, Table 4). The adopted figure of -70‰ has an approximate uncertainty of ca. 10‰, reflecting the imprecisely known degassing conditions. Within this uncertainty, the mass-balance conclusions outlined in Section 5.3 are robust.

5.6. Implications for the interpretation of speleothem calcite $\delta^{13}\text{C}$ values

We have demonstrated that $\delta^{13}\text{C}_{\text{DIC}}$ values of the dripwater at Grotta di Ernesto do not directly reflect the C isotopic composition of the soil waters, but are altered by carbonate dissolution in the soil and epikarst and by degassing prior to reaching the stalagmite surface. A rise of approximately 1.5‰ in the $\delta^{13}\text{C}_{\text{DIC}}$ is attributed to closed-system dissolution. This proportion can vary in different caves and, thus, needs to be determined on a site by

site basis. An additional increase of 1–1.5‰ is attributed to rapid kinetic degassing of aqueous CO_2 upon entering the cave chamber. The ^{13}C enrichment is higher in the two slower drips compared to the faster one and we can now confidently attribute this to kinetically enhanced degassing of isotopically light carbon dioxide due to the pCO_2 gradient which is driven by advective air flow in the cold season (by considering that the initial pCO_2 of the winter water remains about $10^{-2.8}$ (1600 ppm), but the variation in cave pCO_2 is large). Furthermore, speleothem calcite is isotopically heavier by about 5‰ relative to the initial water C isotopic composition (Table 4). This enrichment in the heavier isotope can be related to further degassing at the impact point (where the drop fragments upon contact with the speleothem), followed by continued degassing of the solution film wetting the top of the stalagmite towards equilibration with cave air pCO_2 .

Fig. 14 illustrates the evolution of the $\delta^{13}\text{C}$ values from the initial water C isotope composition to that of the final calcite precipitate ($\delta^{13}\text{C}_c$) forming on top of the speleothem under winter conditions. The strong kinetically enhanced effects that have been quantified by the C mass-balance modelling for Grotta di Ernesto overwhelm the small degree of ^{13}C -enrichment resulting from equilibrium degassing on top of the stalagmite. In addition, the expected evolution of $\delta^{13}\text{C}$ in the solution layer on top of a stalagmite (and, thus, in the calcium carbonate) is presented. Provided that the solution has reached complete equilibration with the cave air in ventilated caves, a ^{13}C -enrichment of cave calcite precipitated at the top of a stalagmite (in the zone proximal to the vertical growth axis) is likely due to

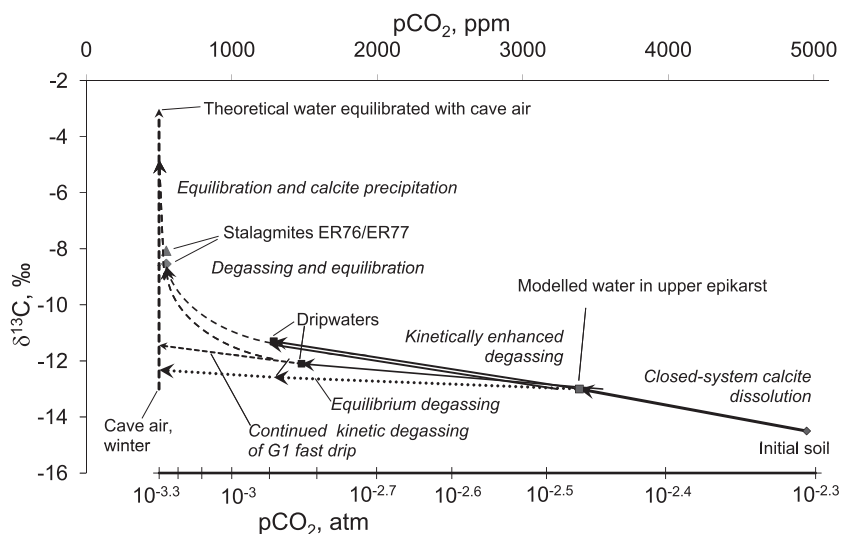


Fig. 14. Scheme explaining the C isotope evolution from dripwater to speleothem at Grotta di Ernesto. The first shift toward relatively high $\delta^{13}\text{C}$ values occurs at the interface between soil and epikarst. Radiocarbon evidence shows that ca. 10% of the C comes from the bedrock implying a stage of closed-system dissolution as water passes from the base of the soil zone into the top of the epikarst. The dripwater is supersaturated because of degassing, but it can be back-tracked to a previous state of initial water in the epikarst which is just at saturation. During degassing $\delta^{13}\text{C}$ increases beyond equilibrium and this is more pronounced in the more degassed slow drips ER76 and ER77 as compared to the fast drip ER G1st-1. The composition of stalagmite-top calcite is significantly more enriched in ^{13}C which is attributed to further CO_2 -loss whereby the kinetic loss is augmented by isotope exchange with cave air. Dripwater remaining in the cave for an extended period is modified by calcite precipitation, leading to higher $\delta^{13}\text{C}$ values and further equilibration towards the limit shown at ca. -3‰ .

a strong gradient between drip and cave air $p\text{CO}_2$ and, to a lesser extent, due to equilibration with cave air, and/or soil processes.

Theoretical models of stalagmite $\delta^{13}\text{C}$ evolution proposed to date do not account for all the complexities related to kinetically enhanced degassing of dripwater prior to forming the solution film on the top of a stalagmite (Mühlinghaus et al., 2007; Dreybrodt, 2008; Mühlinghaus et al., 2009; Scholz et al., 2009). In these models, most of the change in the $\delta^{13}\text{C}$ values of stalagmite calcite can be related to drip rate (Mühlinghaus et al., 2008) and to the residence time of the solution on the surface the stalagmite (Mühlinghaus et al., 2009). For Grotta di Ernesto, we believe that changes in $\delta^{13}\text{C}_{\text{DIC}}$ of the solution film are related to the degree of effective host-rock dissolution and kinetically enhanced degassing. Consequently, the drip rate cannot be reconstructed in ventilated caves by back modelling if these processes are not accounted for.

Our model of C fluxes suggests that the strongest kinetically enhanced degassing occurs at Grotta di Ernesto in the cold season, when the CO_2 concentration gradient between water and cave air is highest, which is similar to the processes observed at Obir cave (Spötl et al., 2005). The effects of kinetically enhanced degassing on calcite precipitation were qualitatively recognized by Frisia et al. (2000) and quantified by Miorandi et al. (2010), who estimated that about 80% of the calcite within the cave precipitates from November to April. The remaining 20% mostly forms between May and July. Consequently, the $\delta^{13}\text{C}_\text{c}$ values of stalagmites from Grotta di Ernesto, most likely record the values of the calcite formed when the external temperature is lower than the cave temperature (see Frisia et al., 2005). In winter the initial shift to higher $\delta^{13}\text{C}_{\text{DIC}}$ values of dripwater is rapid, due to kinetically enhanced degassing (Fig. 14). Subsequently degassing occurs at the impact point on the top surface of the stalagmite, followed by equilibration with cave CO_2 and calcite precipitation. The value of -8‰ at the apex of a stalagmite is expected to progressively increase away from the impact point, in particular when the stalagmite is cone-shaped, such as those at Grotta di Ernesto. If the evolution continues towards equilibration with the cave air reservoir (Scholz et al., 2009), and given that the process of calcite precipitation at the temperature of the cave causes enrichment in ^{13}C of HCO_3^- remaining in the solution film (Mook, 2006), the $\delta^{13}\text{C}_\text{c}$ would evolve towards values of up to -3‰ . In summer, the effect of forced kinetic degassing is low, because the difference between cave air and water $p\text{CO}_2$ is smaller than in winter. The contribution to $\delta^{13}\text{C}$ due to calcite precipitation is negligible, because very little calcite forms. The cumulative effect of equilibration with cave air is important, but it shifts the C isotopic composition only by about 1‰ . Equilibration with cave air, in fact, would shift the values of the $\delta^{13}\text{C}_{\text{DIC}}$ of the solution to -11‰ , and this would also be the isotopic value of calcite deposited at the top of the stalagmite from this equilibrated parent solution.

On the basis of the evolution of $\delta^{13}\text{C}$ in the cave waters HCO_3^- it is clear that the $\delta^{13}\text{C}_\text{c}$ values of Grotta di Ernesto stalagmites may be related to the strength or duration of kinetic degassing in addition to soil and epikarst processes,

which are responsible for $p\text{CO}_2$ in the initial water. Thus, at relatively constant soil air $p\text{CO}_2$, low $\delta^{13}\text{C}_\text{c}$ values in Grotta di Ernesto speleothems should be indicative of predominant “summer mode”, which is characterized by less effective kinetic degassing at the stalactite tip and equilibration with the cave air. Higher $\delta^{13}\text{C}_\text{c}$ values should be indicative of a predominant “winter mode”, which is characterized by kinetically enhanced degassing at the stalactite tip followed by further degassing and equilibration with the cave air almost at atmospheric values.

In the light of the new observations and mass-balance modelling for Grotta di Ernesto, we have revisited the study of Obir cave, SE Austria (Spötl et al., 2005). Obir is a dynamically ventilated cave system and shows a similar seasonal range in air $p\text{CO}_2$ composition as Grotta di Ernesto, despite the much greater size and depth of the former cave system. The distribution of $\delta^{13}\text{C}_{\text{DIC}}$ values and ion concentrations in dripwaters at Obir demonstrated that an initial stage of kinetic degassing from soil water compositions occurs, followed by (in different drips and at different times) diverse combinations of further degassing towards cave air $p\text{CO}_2$ values, and calcite precipitation with accompanying CO_2 loss. A comparison with Grotta di Ernesto is instructive. Above Obir cave, soil $\delta^{13}\text{C}$ values are similar to those measured above Grotta di Ernesto (Spötl et al., 2005) and the dead carbon fraction in pre-bomb 20th century carbonates is around 15% (Smith et al., 2009). Carbon isotope compositions for stalagmites Ob12 (-7.9‰) and Obi84 (-7.0‰), fed by dripwater with mean $\delta^{13}\text{C}_{\text{DIC}}$ value of -10.2‰ (Fairchild et al., 2010) indicate a stronger equilibration effect than at Grotta di Ernesto. The interpretation of Smith et al. (2009) who observed that the ^{14}C (bomb-spike) profile of sample Ob84 showed a simultaneous rise in ^{14}C to that in the external atmosphere and attributed this to some equilibration between the dripwater and the cave air is, thus, supported by mass-balance C-isotope modelling. This implies that, when there is equilibration with cave air in ventilated caves, the $\delta^{13}\text{C}$ values of speleothems may directly reflect atmospheric CO_2 changes (see Baskaran and Krishnamurthy, 1993).

The most extreme case of high cave dripwater $\delta^{13}\text{C}_{\text{DIC}}$ values with respect to the soil waters observed at Obir cave is slow drip SH-2 (0.1 drips per minute), which during winter 2001–2002 attained $\delta^{13}\text{C}_{\text{DIC}}$ values as high as -2.9‰ (Spötl et al., 2005). This value was accompanied by a significant degree of prior calcite precipitation, as the DIC values dropped to 60% of their summer values. Application of the Rayleigh fractionation equation, following Bar-Matthews et al. (1996) and Spötl et al. (2005), indicates that nearly 4.8‰ of the rise in $\delta^{13}\text{C}$ can be attributed to equilibrium exchange with cave air. The observed value of -2.9 is almost exactly what is expected from complete equilibration of the solution water with a cave air of a fixed composition of -13‰ (given a fractionation between HCO_3^- and CO_2 of 10.14‰ at 5.5 °C).

Obir cave is significantly larger than Grotta di Ernesto and, most importantly, has openings at different elevations. Although soil conditions and $p\text{CO}_2$ levels in the two caves are comparable, the rate of air exchange is thus much faster in Obir cave which will enhance the isotope exchange process.

6. CONCLUDING REMARKS

Mass-balance modelling of air fluxes in a simple, descending cave devoid of apparent fissures indicates that advection forces air circulation, whereas diffusion is negligible. Air exchange between the cave and the external atmosphere is particularly rapid in the cold season when $p\text{CO}_2$ in the cave air drops to about 500 ppm from the summer maximum (10,000 ppm). We calculated that the average rate of air exchange in winter is less than one day.

Mass-balance calculations indicate that cave CO_2 concentration and its isotopic composition are mostly determined by the influx of soil air into the cave in summer and outflow of warm cave air in winter through fissures in the rock. The most important effect of advection-driven cave ventilation is to force a first phase of kinetically enhanced degassing when the $p\text{CO}_2$ gradient between drip-water and cave air is at a maximum (i.e. in winter). Mass balance modelling constrained by C-isotope data indicates that this process accounts for a very small percentage of isotopically light CO_2 which mixes with the cave air in the cold season. The mass-balance modelling supports the hypothesis that a first phase of relatively fast degassing of ^{13}C -depleted CO_2 without back-reaction prior to the formation of a solution film on top of stalagmites occurs in ventilated caves, as proposed by Dulinski and Rozanski (1990) and Dreybrodt (2008).

At Grotta di Ernesto, prior calcite precipitation is minor, and cannot explain the observed systematic shift toward higher $\delta^{13}\text{C}$ values, from a mean of about -14.5‰ in soil water to a mean of about -8‰ of the speleothem calcite. The carbon isotopic evolution from soil water to cave calcite has been attributed to the following sequence of processes: (i) closed-system dissolution of carbonates in basal soil and epikarst, (ii) an initial phase of kinetically-enhanced degassing, as theoretically implied by Dreybrodt (2008), possibly followed by more degassing at the impact point; (iii) degassing and equilibration of the solution film with cave air as modelled by Scholz et al. (2009). A similar chain of processes explains the carbon isotope evolution from soil to speleothems also for the well-known ventilated cave of Obir and may occur in many other cave systems, particularly those with more than one entrance or with fracture systems cutting through the host rock.

In our model, the initial phase of kinetically enhanced degassing is the most important cave process causing ^{13}C -enrichment of the initial solution (i.e. the original soil water which was modified by carbonate dissolution prior to entering in the cave) as hypothesized by Dulinski and Rozanski (1990).

At Grotta di Ernesto and at Obir caves seasonal changes in air flow modulate the C-fluxes. Consequently, the winter signal dominates the $\delta^{13}\text{C}$ values of calcite as well as other climate-related properties driven by C-fluxes such as the growth rate of speleothems, similar to what was previously inferred for other caves by Genty et al. (2001), Fairchild et al. (2006a) and Baldini et al. (2008).

The most important implication of our modelling for speleothem-based paleoenvironmental studies is that speleothem $\delta^{13}\text{C}$ values higher than expected from equilibrium

fractionation with HCO_3^- derived by equilibration with soil CO_2 and evolved from C3 vegetation may not be uniquely ascribed to climate-related factors such as drip-rate variability and/or soil CO_2 production. Nevertheless, C-isotope values of cave calcite precipitated under the influence of forced cave air circulation may still capture surface processes, provided a thorough study of cave C-fluxes assesses their significance. For example, in the highly ventilated Obir cave, equilibration with the cave atmosphere results in stalagmites whose ^{14}C activity reflects atmospheric changes.

Forced air flow driven by different gas densities appears to be characteristic of ascending and descending caves in geographic locations characterized by marked temperature differences between the cave interior and the free atmosphere. Processes similar to those illustrated for Grotta di Ernesto are potentially common in many mid- and high-latitude caves. The study by Genty et al. (2006) was carried out in at least one cave characterized by forced convection (Bourges et al., 2006). Higher speleothem $\delta^{13}\text{C}$ values were, however, accompanied by diminution and cessation of speleothem growth, and this trend was documented for more than one cave and correlated with ice core data. Genty et al. (2006) interpreted speleothem $\delta^{13}\text{C}$ trends in terms of a shift toward a cold climate and consequent cessation of soil CO_2 production is thus absolutely plausible.

The ultimate conclusion of our study is that the interpretation of speleothem-based climate-proxy time series should be, whenever possible, validated by monitoring data. When there is no possibility to monitor the modern system, independent proxies from the same, or different archives, are needed to verify the climatic interpretation.

ACKNOWLEDGMENTS

This work was supported by DFG Research Group 668 (DAPHNE) co-ordinated by Augusto Mangini, whom we wish to acknowledge for his enthusiastic support. Additional financial contribution (A.B.) came from the AQUAPAST project (funded by Fondo Unico per la Ricerca – Provincia Autonoma di Trento), and NERC project NE/C511805/1 (to I.J.F.). Michele Zandonati helped with artwork and assistance in the field, and Manuela Wimmer's support in the isotope laboratory is greatly appreciated. We are grateful to two anonymous reviewers for providing valuable insight and constructive criticism, which resulted in improvements to the manuscript.

REFERENCES

- Andrews J. (2006) Palaeoclimatic records from stable isotopes in riverine tufas: synthesis and review. *Earth-Sci. Rev.* **75**, 85–104.
- Avanzini M., Frisia S., van den Driessche K. and Keppens E. (1997) A dinosaur tracksite in an Early Liassic tidal flat in northern Italy: palaeoenvironmental reconstruction from sedimentology and geochemistry. *Palaio* **12**, 538–551.
- Baldini J. U. L., Baldini L. M., McDermott F. and Clipson N. (2006) Carbon dioxide sources, sinks, and spatial variability in shallow temperate zone caves: evidence from Ballynamindra Cave, Ireland. *J. Cave Karst Stud.* **68**, 4–11.
- Baldini J. U. L., McDermott F., Hoffmann D. K., Richards D. A. and Clipson N. (2008) Very high-frequency and seasonal cave

- atmosphere pCO₂ variability: implications for stalagmite growth and oxygen isotope-based paleoclimate records. *Earth Planet. Sci. Lett.* **272**, 118–129.
- Bar-Matthews M., Ayalon A., Matthews A., Sass E. and Halicz L. (1996) Carbon and oxygen isotope study of the active water-carbonate system in a karstic Mediterranean cave: implications for palaeoclimate research in semiarid regions. *Geochim. Cosmochim. Acta* **60**, 337–347.
- Bar-Matthews M., Ayalon A. and Kaufman A. (1997) Late Quaternary paleoclimate in the eastern Mediterranean region from stable isotope analysis of speleothems at Soreq Cave. *Israel. Quat. Res.* **47**, 155–168.
- Baskaran M. and Krishnamurthy R. V. (1993) Speleothems as proxy for the carbon isotope composition of atmospheric CO₂. *Geophys. Res. Lett.* **20**, 2905–2908.
- Berner R. A. (2006) GEOCARBSULF: a combined model for Phanerozoic atmospheric O₂ and CO₂. *Geochim. Cosmochim. Acta* **70**, 5653–5664.
- Borsato A. (1997) Dripwater monitoring at Grotta di Ernesto (NE-Italy): a contribution to the understanding of karst hydrology and the kinetics of carbonate dissolution. In *Proceedings of Sixth Conference on Limestone Hydrology and Fissured Media*, vol. 2. La Chaux de Fonds, Switzerland, pp. 57–60.
- Bourges F., Genthon P., Mangin A. and d'Hulst D. (2006) Microclimates of L'Aven d'Ornac and other French limestone caves (Chauvet, Esparros, Marsoulas). *Int. J. Climatol.* **26**, 1651–1670.
- Cerling T. E. (1984) The stable isotopic composition of soil carbonate and its relationship to climate. *Earth Planet. Sci. Lett.* **71**, 229–240.
- Cerling T. E., Wang Y. and Quade J. (1993) Expansion of C4 ecosystems as an indicator of global ecological change in the late Miocene. *Nature* **361**, 344–345.
- Dorale J. A., González L. A., Reagan M. K., Pickett D. A., Murrell M. T. and Baker R. G. (1992) A high-resolution record of Holocene climate change in speleothem calcite from Cold Water Cave, northeast Iowa. *Science* **258**, 1626–1630.
- Dreybrodt W. (2008) Evolution of the isotopic composition of carbon and oxygen in a calcite precipitating H₂O–CO₂–CaCO₃ solution and the related isotopic composition of calcite in stalagmites. *Geochim. Cosmochim. Acta* **72**, 4712–4724.
- Dulinski M. and Rozanski K. (1990) Formation of ¹³C/¹²C isotope ratios in speleothems: a semi-dynamic model. *Radiocarbon* **32**, 7–16.
- Eccel E. and Saibanti S. (2008) Inquadramento climatico dell'Altopiano di Lavarone-Vezzena nel contesto generale trentino. *Stud. Trent. Sci. Nat. Acta Geol.* **82**, 111–121.
- Egli M., Sartori G., Mirabella A., Favilli F., Giaccari D. and Delbos E. (2009) Effect of north and south exposure on organic matter in high Alpine soils. *Geoderma* **149**, 124–136.
- Ek C. and Gewalt M. (1985) Carbon dioxide in cave atmospheres – new results in Belgium and comparison with some other countries. *Earth Surf. Proc. Land.* **10**, 173–187.
- Faimon J., Stelcl J. and Sas D. (2006) Anthropogenic CO₂-flux into cave atmosphere and its environmental impact: a case study in the Císařská Cave (Moravian Karst, Czech Republic). *Sci. Total Environ.* **369**, 231–245.
- Fairchild I. J., Borsato A., Tooth A., Frisia S., Hawkesworth C. J., Huang Y., McDermott F. and Spiro B. (2000) Control on trace element (Sr–Mg) compositions of carbonate cave water: implications for speleothem climatic records. *Chem. Geol.* **166**, 255–269.
- Fairchild I. J., Baker A., Borsato A., Frisia S., Hinton R. W., McDermott F. and Tooth A. (2001) Annual to sub-annual resolution of multiple trace-element trends in speleothems. *J. Geol. Soc. Lond.* **158**, 831–841.
- Fairchild I. J., Smith C. L., Baker A., Fuller L., Spötl C., Matthey D. and McDermott F.E.I.M.F. (2006a) Modification and preservation of environmental signals in speleothems. *Earth Sci. Rev.* **75**, 105–153.
- Fairchild I. J., Tuckwell G. W., Baker A. and Tooth A. F. (2006b) Modelling of dripwater hydrology and hydrogeochemistry in a weakly karstified aquifer (Bath, UK): implications for climate change studies. *J. Hydrol.* **321**, 213–231.
- Fairchild I. J., Frisia S., Borsato A. and Tooth A. F. (2007) Speleothems. In *Geochemical Sediments and Landscapes* (eds. D. J. Nash and S. J. McLaren). Blackwells, Oxford, pp. 200–245.
- Fairchild I. J., Loader N. J., Wynn P. M., Frisia S., Thomas P. A., Lagueard J. G. A., de Momi A., Hartland A., Borsato A., La Porta N. and Susini J. (2009) Sulfur fixation in wood mapped by synchrotron X-ray studies: implications for environmental archives. *Environ. Sci. Technol.* **43**, 1310–1315.
- Fairchild I. J., Spötl C., Frisia S., Borsato A., Susini J., Wynn P. M., Cauzid J. and EIMF. (2010) Petrology and geochemistry of annually laminated stalagmites from an Alpine cave (Obir, Austria): seasonal cave physiology. In *Tufas and Speleothems: Unravelling the Microbial and Physical Controls*, vol. 336 (eds. H. M. Pedley and M. Rogerson). Geological Society, London, Special Publication, pp. 295–321.
- Fernandez-Cortes A., Sanchez-Moral S., Cuezva S., Cañaveras J. C. and Abella R. (2009) Annual and transient signatures of gas exchange and transport in the Castañar de Ibor cave (Spain). *Int. J. Speleol.* **38**, 153–162.
- Fohlmeister J., Schröder-Ritzrau A., Spötl C., Frisia S., Miorandi R., Kromer B. and Mangini A. (2010) The influences of hydrology on the radiogenic and stable carbon isotope composition of cave drip water, Grotta di Ernesto (Italy). *Radiocarbon* **54**, in press.
- Fohlmeister J., Kromer B. and Mangini A. (in press) The influence of soil organic matter age spectrum on the reconstruction of atmospheric ¹⁴C levels via stalagmites. *Radiocarbon*.
- Frisia S. and Wenk H. R. (1993) TEM and AEM study of pervasive multi-step dolomitization of the Upper Triassic Dolomia Principale Northern Italy). *J. Sedim. Petrol.* **63**, 1049–1058.
- Frisia S., Borsato A., Fairchild I. J. and McDermott F. (2000) Calcite fabrics, growth mechanisms, and environments of formation in speleothems from the Italian Alps and southwestern Ireland. *J. Sedim. Res.* **70**, 1183–1196.
- Frisia S., Borsato A., Preto N. and McDermott F. (2003) Late Holocene annual growth in three Alpine stalagmites records the influence of solar activity and the North Atlantic Oscillation on winter climate. *Earth Planet. Sci. Lett.* **216**, 411–424.
- Frisia S., Borsato A., Fairchild I. J. and Susini J. (2005) Variations in atmospheric sulphate recorded in stalagmites by synchrotron micro XRF and XANES analyses. *Earth Planet. Sci. Lett.* **235**, 729–740.
- Genty D. and Massault M. (1999) Carbon transfer dynamics from bomb ¹⁴C and δ¹³C time series of a laminated stalagmite from SW France – modeling and comparison with other stalagmite records. *Geochim. Cosmochim. Acta* **63**, 1537–1548.
- Genty D., Baker A. and Vokal B. (2001) Intra- and inter-annual growth rate of modern stalagmites. *Chem. Geol.* **176**, 191–212.
- Genty D., Blamart D., Ouahdi R., Gilmour M., Baker A., Jouzel J. and Van-Exter S. (2003) Precise dating of Dansgaard–Oeschger climate oscillations in western Europe from stalagmite data. *Nature* **421**, 833–837.
- Genty D., Blamart D., Ghaleb B., Plagnes V., Causse Ch., Bakalowicz M., Zouari K., Chkir N., Hellstrom J., Wainer K. and Bourges F. (2006) Timing and dynamics of the last deglaciation from European and North African δ¹³C stalagmite

- profiles – comparisons with Chinese and South Hemisphere stalagmites. *Quat. Sci. Rev.* **25**, 2118–2142.
- Haki J., Hunyadi I., Csige I., Géczy G., Lénart K. L. and Várhegyi A. (1997) Radon transport phenomena studied in karst caves – international experiences on radon levels and exposures. *Radiat. Meas.* **28**, 675–684.
- Hendy C. (1971) The isotopic geochemistry of speleothems – I. The calculation of the effects of different modes of formation on the isotopic composition of speleothems and their applicability as palaeo-climate indicators. *Geochim. Cosmochim. Acta* **35**, 801–824.
- Huang Y. and Fairchild I. J. (2001) Partitioning of Sr²⁺ and Mg²⁺ into calcite under karst-analogue experimental conditions. *Geochim. Cosmochim. Acta* **65**, 47–62.
- Huang Y., Fairchild I. J., Borsato A., Frisia S., Cassidy N. J., McDermott F. and Hawkesworth C. J. (2001) Seasonal variations in Sr, Mg and P in modern speleothems (Grotta di Ernesto, Italy). *Chem. Geol.* **175**, 429–448.
- Kaufmann G. (2003) Stalagmite growth and palaeo-climate: the numerical perspective. *Earth Planet. Sci. Lett.* **214**, 251–266.
- Kivastik J. (1998) Paediatric reference values for spirometry. *Clin. Physiol.* **18**, 489–497.
- Kluge T., Riechelmann D. F. C., Wieser M., Spötl C., Sültenfuß J., Schröder-Ritzrau A., Niggemann S. and Aeschbach-Hertig W. (2010) Dating cave drip water by tritium. *J. Hydrol.* doi:10.1016/j.jhydrol.2010.09.015.
- Lachniet M. S. (2009) Climatic and environmental controls on speleothem oxygen-isotope values. *Quat. Sci. Rev.* **28**, 412–432.
- Leifeld J. and Fuhrer J. (2005) The temperature response of CO₂ production from bulk soils and soil fractions is related to soil organic matter quality. *Biogeochemistry* **75**, 433–453.
- Leng M. J. and Marshall J. D. (2004) Palaeoclimate interpretation of stable isotope data from lake sediment archives. *Quat. Sci. Rev.* **23**, 811–831.
- Marcolla B., Cescatti A., Montagnani L., Manca G., Kerschbaumer G. and Minerbi S. (2005) Importance of advection in the atmospheric CO₂ exchanges of an alpine forest. *Agric. Forest Meteorol.* **130**, 193–196.
- McDermott F. (2004) Palaeo-climate reconstruction from stable isotope variations in speleothems: a review. *Quat. Sci. Rev.* **23**, 901–918.
- McDermott F., Frisia S., Yiming H., Longinelli A., Spiro B., Heaton T. H. E., Hawkesworth C. J., Borsato A., Keppens E., Fairchild I. J., van der Borg K., Verheyden S. and Selmo E. (1999) Holocene climate variability in Europe: evidence from $\delta^{18}\text{O}$, textural and extension-rate variations in three speleothems. *Quat. Sci. Rev.* **18**, 1021–1038.
- McDermott F., Schwarcz H. and Rowe P. J. (2005) Isotopes in speleothems. In *Isotopes in Palaeoenvironmental Research* (ed. M. J. Leng). Springer, Amsterdam, pp. 185–225.
- Miorandi R., Borsato A. and Frisia S. (2006) Long-term drip-rate monitoring at Grotta di Ernesto (Trentino, NE Italy): hydrological aspects. In *Proceedings of the Symposium Climate Change: The Karst Record (IV) Baile Herculane*, vol. 10. Romania Karst Waters Institute, Special Publication, pp. 20–22.
- Miorandi R., Borsato A., Frisia S., Fairchild I. J. and Richter D. (2010) Long term drip-water monitoring and CaCO₃ precipitation in a shallow cave (Grotta di Ernesto, N. Italy): epikarst hydrology and implications for speleothem growth and paleo-climate reconstructions. *Hydrol. Processes* **24**, 3101–3114.
- Mook W. G. (2006) *Introduction to Isotope Hydrology*. Taylor and Francis, London.
- Mook W. G. and de Vriess J. (2000) Introduction. Theory, Methods, Review. In *Environmental Isotopes in the Hydrological Cycle. Principles and Applications*, vol. 1. IAEA.
- Mook W. G., Bommerson J. and Staverman W. (1974) Carbon isotope fractionation between dissolved bicarbonate and gaseous carbon dioxide. *Earth Planet. Sci. Lett.* **22**, 169–176.
- Mühlinghaus C., Scholz D. and Mangini A. (2007) Modelling stalagmite growth and $\delta^{13}\text{C}$ as a function of drip interval and temperature. *Geochim. Cosmochim. Acta* **71**, 2780–2790.
- Mühlinghaus C., Scholz D. and Mangini A. (2008) Temperature and precipitation records from stalagmites grown under disequilibrium conditions. *PAGES News* **16**, 19–20.
- Mühlinghaus C., Scholz D. and Mangini A. (2009) Modelling fractionation of stable isotopes in stalagmites. *Geochim. Cosmochim. Acta* **73**, 7275–7289.
- Romanov D., Kaufmann G. and Dreybrodt W. (2008) $\Delta^{13}\text{C}$ profiles along growth layers of stalagmites. *Geochim. Cosmochim. Acta* **72**, 438–448.
- Salomons W. and Mook W. G. (1986) Isotope geochemistry of carbonates in the weathering zone. In *Handbook of Environmental Isotope Geochemistry 2, The Terrestrial Environment, 2B* (eds. P. Fritz and J. Ch. Fontes). Elsevier, Amsterdam, pp. 239–270.
- Scholz D., Mühlinghaus C. and Mangini A. (2009) Modelling $\delta^{13}\text{C}$ and $\delta^{18}\text{O}$ in the solution layer on stalagmite surfaces. *Geochim. Cosmochim. Acta* **73**, 2592–2602.
- Shackleton N. J., Hall M. A., Line J. and Crag S. (1983) Carbon isotope data in core V19–30 confirm reduced carbon dioxide concentration in the ice age atmosphere. *Nature* **306**, 319–322.
- Smith C. L., Baker A., Fairchild I. J., Frisia S. and Borsato A. (2006) Reconstructing hemispheric-scale climates from multiple stalagmite records. *Int. J. Climatol.* **26**, 1417–1424.
- Smith C. L., Fairchild I. J., Spötl C., Frisia S., Borsato A., Moreton S. G. and Wynn P. M. (2009) Chronology-building using objective identification of annual signals in trace element profiles of stalagmites. *Quat. Geochron.* **4**, 11–21.
- Spötl C. (2004) A simple method of soil gas stable carbon isotope analysis. *Rapid Comm. Mass. Spectrom.* **18**, 1239–1242.
- Spötl C. (2005) A robust and fast method of sampling and analysis of $\delta^{13}\text{C}$ of dissolved inorganic carbon in ground waters. *Isot. Environ. Health Stud.* **41**, 217–221.
- Spötl C., Fairchild I. J. and Tooth A. F. (2005) Cave air control on dripwater geochemistry, Obir Caves (Austria): Implications for speleothem deposition in dynamically ventilated caves. *Geochim. Cosmochim. Acta* **69**, 2451–2468.
- Thorntonwaite C. W. and Mather J. R. (1955) The water balance. *Publ. Climatol.* **8**, 1–104.
- Troester J. W. and White B. W. (1984) Seasonal fluctuations in the carbon dioxide partial pressure in a cave atmosphere. *Water Res. Res.* **20**, 153–156.
- Urbanc J., Trček B., Pezdič J. and Lojen S. (1997) Dissolved carbon isotope composition of waters. *Acta Carsol.* **26**, 236–259.
- Wynn P. M., Fairchild I. J., Frisia S., Spötl C., Baker A., Borsato A. and MF E. I. (2010) High-resolution sulphur isotope analysis of speleothem carbonate by secondary ionization mass spectrometry. *Chem. Geol.* **271**, 101–107.